IMMUNOLOGY

SRSF1 serves as a critical posttranscriptional regulator at the late stage of thymocyte development

Zhihong Qi[1†], Fang Wang[1†], Guotao Yu[1†], Di Wang[2†], Yingpeng Yao[1], Menghao You[1], Jingjing Liu[1], Juanjuan Liu[1], Zhen Sun[1], Ce Ji[1], Yuanchao Xue[2], Shuyang Yu[1]*

The underlying mechanisms of thymocyte maturation remain largely unknown. Here, we report that serine/arginine-rich splicing factor 1 (SRSF1) intrinsically regulates the late stage of thymocyte development. Conditional deletion of SRSF1 resulted in severe defects in maintenance of late thymocyte survival and a blockade of the transition of TCRβ^{hi}CD24^{+}CD69^{+} immature to TCRβ^{hi}CD24^{-}CD69^{-} mature thymocytes, corresponding to a notable reduction of recent thymic emigrants and diminished periphery T cell pool. Mechanistically, SRSF1 regulates the gene networks involved in thymocyte differentiation, proliferation, apoptosis, and type I interferon signaling pathway to safeguard T cell intrathymic maturation. In particular, SRSF1 directly binds and regulates *Irf7* and *Il-27ra* expression via alternative splicing in response to type I interferon signaling. Moreover, forced expression of interferon regulatory factor 7 rectifies the defects in SRSF1-deficient thymocyte maturation via restoring expression of type I interferon–related genes. Thus, our work provides new insight on SRSF1-mediated posttranscriptional regulatory mechanism of thymocyte development.

INTRODUCTION

Intrathymic T cell precursors undergo a step-wise development, originating from CD4^{-}CD8^{-} double-negative (DN) thymocytes—which can be further subcategorized into DN1, DN2, DN3, and DN4 subsets by tracking the expression of surface markers CD25 and CD44—and then differentiate into the CD4^{+}CD8^{+} double-positive (DP) cells (*1*). Those DP thymocytes expressing αβ T cell receptors (αβTCRs) that can interact with major histocompatibility complex (MHC) molecules undergo positive selection, resulting in commitment and differentiation into either CD4^{+}CD8^{-} or CD4^{-}CD8^{+} single-positive (SP) thymocytes, respectively (*2*, *3*). Both DP and SP thymocytes with high affinity for TCR-peptide-MHC interaction are forced into negative selection, also termed as clonal deletion by apoptosis, or diverted into alternative lineages, for example, Foxp3^{+} regulatory T cells (*4*). SP thymocytes that survive these processes must still undergo a series of steps for final maturation before they gain functional competency and enter the periphery T cell pool (*5*).

The dynamic alterations of surface markers associated with functional changes are important for understanding the molecular mechanisms guiding T cell intrathymic maturation. For instance, the expression of Qa2 and CD24 (also called heat-stable antigen) is used to define the maturation degree of thymocytes (*6*–*9*). According to the expression of CD24 and CD69, TCRβ^{hi} thymocytes can be further subdivided into TCRβ^{hi}CD69^{+}CD24^{+} immature and TCRβ^{hi}CD69^{-}CD24^{-} mature populations. The TCRβ^{hi}CD69^{+}CD24^{+} immature cells are composed of four subsets, including post-selection DP thymocytes, CD4^{+}CD8^{lo} intermediate cells (IMs), and immature CD4 SP and CD8 SP thymocytes, whereas the TCRβ^{hi}CD69^{-}CD24^{-} mature population contains mature CD4 and CD8 SP subsets (*10*). During the transition from immature to mature thymocytes, the expression of Qa2, CD62L, and sphingosine 1–phosphate receptor 1 (S1PR1) is up-regulated accompanied with CD69 and CD24 down-regulation to access the emigration (*11*). The transition of thymocytes throughout the processes of maturation is dependent on signals transmitted by TCR, cytokine receptors, and various cell surface molecules (*12*, *13*), which are critical to successfully sustain their differentiation, antiapoptosis, and proliferation. Over the decades, accumulating studies have shown that a series of mediators are required for these processes, which are largely involved in nuclear factor κB signaling pathway (*14*). A recent work by Xing and colleagues (*15*) reported that type I interferon signaling is correlated with terminal maturation via up-regulating signal transducer and activator of transcription 1 (STAT1) and interferon regulatory factor 7 (IRF7) expression and promoting the surface Qa2 expression, which provided a new insight into T cell maturation in response to type I interferon signal. However, the complicated mechanisms of T cell terminal maturation are rarely understood.

Serine/arginine-rich splicing factor 1 (SRSF1; also known as SF2/ASF) is a pivotal posttranscriptional regulator for gene expression in various biological processes (*16*). A recent study demonstrated the essential roles of SRSF1 in controlling T cell hyperactivity and systemic autoimmunity (*17*). However, the roles of SRSF1 involved in thymocyte development remain unknown. In this study, we report that conditional ablation of SRSF1 in DP thymocytes leads to substantial defects on terminal maturation. We further verified that SRSF1 promotes proliferation and survival of thymocytes by modulating the T cell regulatory networks posttranscriptionally. In particular, SRSF1 controls the abundances of *Il27ra* and *Irf7* via alternative splicing (AS), which are critical in response to type I interferon signaling for supporting thymocyte maturation.

RESULTS

SRSF1 plays critical roles in the late stage of thymocyte development

To elucidate the function of SRSF1 in the late stage of thymocyte development, we crossed *Srsf1*$^{fl/fl}$ mice (*18*) with *Lck*-Cre mice (*19*), which drives the Cre recombinase expression by proximal Lck promoter (*20*) and effectively deletes the floxed gene fragment at the DP stage (*21*, *22*), to conditionally inactivate SRSF1 (Fig. 1A). The

[1]State Key Laboratory of Agrobiotechnology, College of Biological Sciences, China Agricultural University, Beijing 100193, China. [2]Key Laboratory of RNA Biology, CAS Center for Excellence in Biomacromolecules, Institute of Biophysics, Chinese Academy of Sciences, Beijing 100101, China.
†These authors contributed equally to this work.
*Corresponding author. Email: ysy@cau.edu.cn

expression of SRSF1 at mRNA (fig. S1A) and protein levels (fig. S1B) was determined in distinct subsets including DN3, DN4, ISP, DP, $CD4^+$ SP, and $CD8^+$ SP thymocytes of $Srsf1^{fl/fl}Lck^{Cre/+}$ mice and littermate $Srsf1^{fl/fl}$ (henceforth called control) mice as controls. The results indicated that SRSF1 was initially ablated from the immature single-positive (ISP) stage and effectively deleted in DP and SP thymocytes from $Srsf1^{fl/fl}Lck^{Cre/+}$ mice. Compared with controls, $Srsf1^{fl/fl}Lck^{Cre/+}$ mice exhibited normal size and cellularity of thymus (Fig. 1B). The frequency and cell numbers of both $CD4^+$ and $CD8^+$ thymocytes from SRSF1-deficient mice were substantially decreased (Fig. 1, C and D). Whereas no statistical difference in absolute numbers of DP and DN thymocytes was observed, there was a notable increase in the frequency of these two subsets (Fig. 1, C and D). Since SRSF1 was not deleted in DN3 and DN4 subsets (fig. S1, A and B), $Srsf1^{fl/fl}Lck^{Cre/+}$ mice exhibited normal early T cell development and TCRβ rearrangement in DN3 and DN4 subsets (fig. S1, C to F).

We next focused on the postselection $TCR\beta^{hi}$ thymocytes. The frequency and cell numbers of $TCR\beta^{hi}$ thymocytes (top row in Fig. 1, E and F) and $TCR\beta^{hi}CD69^-CD24^-$ mature subset (second row in Fig. 1, E and F) were decreased by ~50% or more from $Srsf1^{fl/fl}Lck^{Cre/+}$ mice compared with those from controls. The frequency of $TCR\beta^{hi}CD69^+CD24^+$ immature T cell exhibited a relative increase, but the numbers were remarkably diminished (second row in Fig. 1, E and F). We further analyzed the subpopulations via the expression of CD4 and CD8, reflecting the subsequent developmental processes. Among the $TCR\beta^{hi}CD69^+CD24^+$ immature subsets, the percentages of DP, $CD4^+CD8^{lo}$ IMs, and $CD4^+$ SP subsets were not significantly alerted, but the absolute numbers of these subsets were remarkably decreased in $Srsf1^{fl/fl}Lck^{Cre/+}$ mice (third row in Fig. 1, E and F). Both frequency and absolute numbers of $CD8^+$ SP in $TCR\beta^{hi}CD69^+CD24^+$ immature subset were notably reduced in $Srsf1^{fl/fl}Lck^{Cre/+}$ mice (third row in Fig. 1, E and F). In SRSF1-deficient $TCR\beta^{hi}CD69^-CD24^-$ mature population, the numbers of $CD4^+$ and $CD8^+$ SP were markedly diminished, although the frequency of $CD4^+$ SP was increased, whereas the frequency of $CD8^+$ SP was reduced (bottom row in Fig. 1, E and F). Moreover, $TCR\beta^{hi}CD4^+CD69^-Qa2^+$ and $TCR\beta^{hi}CD8^+CD69^-Qa2^+$ mature thymocytes from $Srsf1^{fl/fl}Lck^{Cre/+}$ mice were substantially decreased (Fig. 1, G and H). To exclude the possible effects of *Lck*-Cre transgene on thymocyte development, we next performed the phenotypic assay from littermates $Srsf1^{fl/fl}$, $Lck^{Cre/+}$ (*Lck*-Cre transgene heterozygous), and $Srsf1^{fl/fl}Lck^{Cre/+}$ mice, respectively. The $Lck^{Cre/+}$ mice exhibited normal thymocyte development compared with that in control mice, whereas defective phenotype was only detected in $Srsf1^{fl/fl}Lck^{Cre/+}$ mice (fig. S1, G and H). These data indicated that aberrant development of thymocytes in $Srsf1^{fl/fl}Lck^{Cre/+}$ mice was attributed to SRSF1 deficiency, but it was irrelevant to heterozygous *Lck*-Cre transgene. Collectively, these results suggest that SRSF1 is essential for the late stage of T cell development and terminal maturation of SP thymocytes.

Ablation of SRSF1 impairs recent thymic emigrants and the peripheral T cell pool

We next investigated whether the peripheral T cell pool was affected in $Srsf1^{fl/fl}Lck^{Cre/+}$ mice. The spleen exhibited normal size, but total cell numbers of spleen were noticeably decreased in $Srsf1^{fl/fl}Lck^{Cre/+}$ mice (Fig. 2A). Both size and cell numbers of lymph nodes (LNs) from $Srsf1^{fl/fl}Lck^{Cre/+}$ mice were substantially reduced compared with those from controls (Fig. 2A). Correspondingly, the mature $CD4^+$ and $CD8^+$ T cell populations in spleens, LNs, and peripheral blood cells (PBCs) were remarkably diminished in $Srsf1^{fl/fl}Lck^{Cre/+}$ mice (Fig. 2, B and C). The residual peripheral T cells in spleen from SRSF1-deficient mice were predominantly $CD44^{hi}CD62L^{lo}$ subset (fig. S2, A and B), exhibiting an activated/effector phenotype, which is generally associated with "homeostatic" expansion owing to lymphopenia (*23*). We further confirmed that the remaining T cells in spleen are "escapees" without effective deletion of SRSF1 (fig. S2C). Given that aberrant thymocyte emigration is one of the crucial factors contributing to impaired peripheral mature T cell pool (*11*, *24*), we set up mice models to directly trace the recent thymic emigrants (RTEs) in vivo by crossing $Srsf1^{fl/fl}Lck^{Cre/+}$ or control mice to RAG2p-GFP (green fluorescent protein) transgenic mice (termed as $Rag2^{GFP}$ mice), which were applied for identifying the RTEs in periphery based on GFP expression (*25*). We observed that both the frequency and absolute numbers of RTEs were markedly decreased in spleens, LNs, and PBCs from $Srsf1^{fl/fl}Lck^{Cre/+}Rag2^{GFP}$ mice in comparison with those from $Rag2^{GFP}$ mice (Fig. 2, D to F). Expression of molecules related to migration such as CD62L, CCR7, and S1PR1 was determined in $TCR\beta^{hi}CD69^-CD24^-$ mature thymocytes. We found that all three makers had no altered expression in $TCR\beta^{hi}CD69^-CD24^-CD4^+$ SP thymocytes, and S1PR1 expression was not changed in $TCR\beta^{hi}CD69^-CD24^-CD8^+$ SP thymocytes from $Srsf1^{fl/fl}Lck^{Cre/+}$ mice. Whereas CD62L expression was down-regulated, CCR7 expression was up-regulated in SRSF1-deficient $TCR\beta^{hi}CD69^-CD24^-CD8^+$ SP thymocytes, respectively (fig. S2, D and E). We further performed analysis of the RTEs in spleen. Although most RTEs kept the naïve status right after egress from the thymus, the percentage of naïve RTEs ($CD44^{lo}CD62L^{hi}$) was still lower in $Srsf1^{fl/fl}Lck^{Cre/+}Rag2^{GFP}$ mice than that in littermate $Rag2^{GFP}$ mice, whereas the frequency of activated RTEs ($CD44^{lo}CD62L^{hi}$) was elevated due to SRSF1 deficiency (fig. S2, F and G). However, the absolute numbers of both naïve and activated RTEs were notably diminished due to the ablation of SRSF1 (fig. S2G). Meanwhile, the SRSF1-deficient splenic RTEs retained efficient deletion of SRSF1 (fig. S2H) and exhibited elevated apoptosis (fig. S2, I and J), resulting in failure to replenish the peripheral T cell pool. Collectively, SRSF1 deficiency resulted in notably diminished RTEs and impaired peripheral T cell pool.

SRSF1 is critical for survival of postselection thymocytes and proliferation of mature thymocytes

Given the elevated apoptosis in SRSF1-deficient RTEs, we extended the apoptosis assay in distinct subsets of postselection $TCR\beta^{hi}$ thymocytes during the maturation from $CD69^+CD24^+$ to $CD69^-CD24^-$ thymocytes. We found that the percentages of annexin V^+ cells were substantially increased in all subsets of $TCR\beta^{hi}$ thymocytes (Fig. 3, A and B), indicating that SRSF1 is crucial for survival of thymocytes during the late stage development. To determine the role of SRSF1 in thymocyte proliferation, we performed 5-bromo-2′-deoxyuridine (BrdU) incorporation assay in DP and mature thymocytes. We found that SRSF1 deficiency leads to a substantial defect in proliferation of mature $CD4^+$ SP and $CD8^+$ SP thymocytes but does not affect the expansion in both $TCR\beta^{lo}CD69^-CD4^+CD8^+$ pre-DP cells and $TCR\beta^{hi}CD69^+CD24^+CD4^+CD8^+$ post-DP cells (Fig. 3, C and D). These results indicated that SRSF1 deficiency specially caused defects in proliferation of mature thymocytes before egress. Given that interleukin-7 (IL-7) signaling is essential for T cell survival and proliferation of the late stage of thymocyte subpopulations (*26*), IL-7Rα is down-regulated in DP thymocytes but up-regulated in SP thymocytes (*27*). We then detected IL-7Rα expression in mature

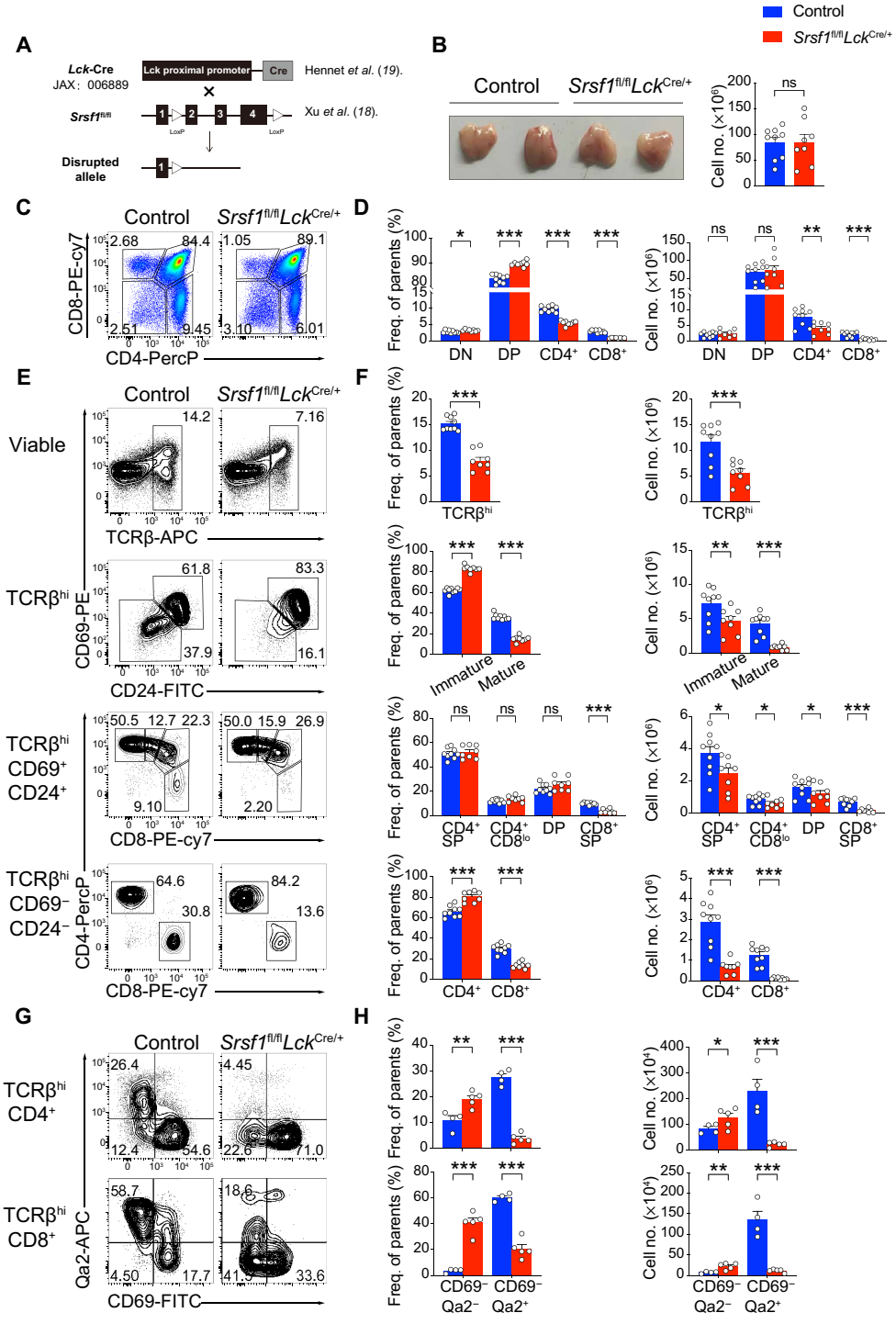

Fig. 1. SRSF1 is critical for T cell late stage development. (**A**) *Lck*-Cre (proximal) mice were crossed with *Srsf1*$^{fl/fl}$ strain to generate conditional knockout mice. Exons 2, 3, and 4 of the *Srsf1* gene flanked by LoxP sites were removed after recombination to inactivate the SRSF1. (**B**) Thymus images and total cell numbers of thymocytes from control ($n = 9$) and *Srsf1*$^{fl/fl}$*Lck*$^{Cre/+}$ ($n = 8$) mice. Photo credit: Z. Qi, China Agricultural University. (**C**) Representative pseudocolor plot shows classic subsets of thymocytes with CD4 and CD8 staining. (**D**) Frequency and numbers of DN, DP, CD4$^+$, and CD8$^+$ thymocytes are statistically shown, respectively (control: $n = 9$; *Srsf1*$^{fl/fl}$*Lck*$^{Cre/+}$: $n = 8$). (**E**) Characterization of postselection thymocytes. TCRβ^{hi} thymocytes (top row) were detected by flow cytometry and further fractionated into CD69$^+$CD24$^+$ immature and CD69$^-$CD24$^-$ mature subsets (second row). The immature subsets were subdivided into CD4$^+$ SP, CD4$^+$CD8^{lo}, DP, and CD8$^+$ SP populations (clockwise from top left in the third row), and the mature subsets were further subdivided into CD4$^+$ and CD8$^+$ populations (bottom row). (**F**) Frequency and numbers of indicated subsets are shown accordingly (control: $n = 9$; *Srsf1*$^{fl/fl}$*Lck*$^{Cre/+}$: $n = 8$). (**G**) Qa2 and CD69 expression on TCRβ^{hi} SP thymocytes. (**H**) Frequency and numbers of Qa2$^-$CD69$^-$and Qa2$^+$CD69$^-$ populations of TCRβ^{hi} SP thymocytes are shown, respectively (control: $n = 4$; *Srsf1*$^{fl/fl}$*Lck*$^{Cre/+}$: $n = 5$). Cumulative data are means ± SEM. ns, not statistically significant; *$P < 0.05$, **$P < 0.01$, and ***$P < 0.001$ (Student's *t* test). Data are from at least three independent experiments.

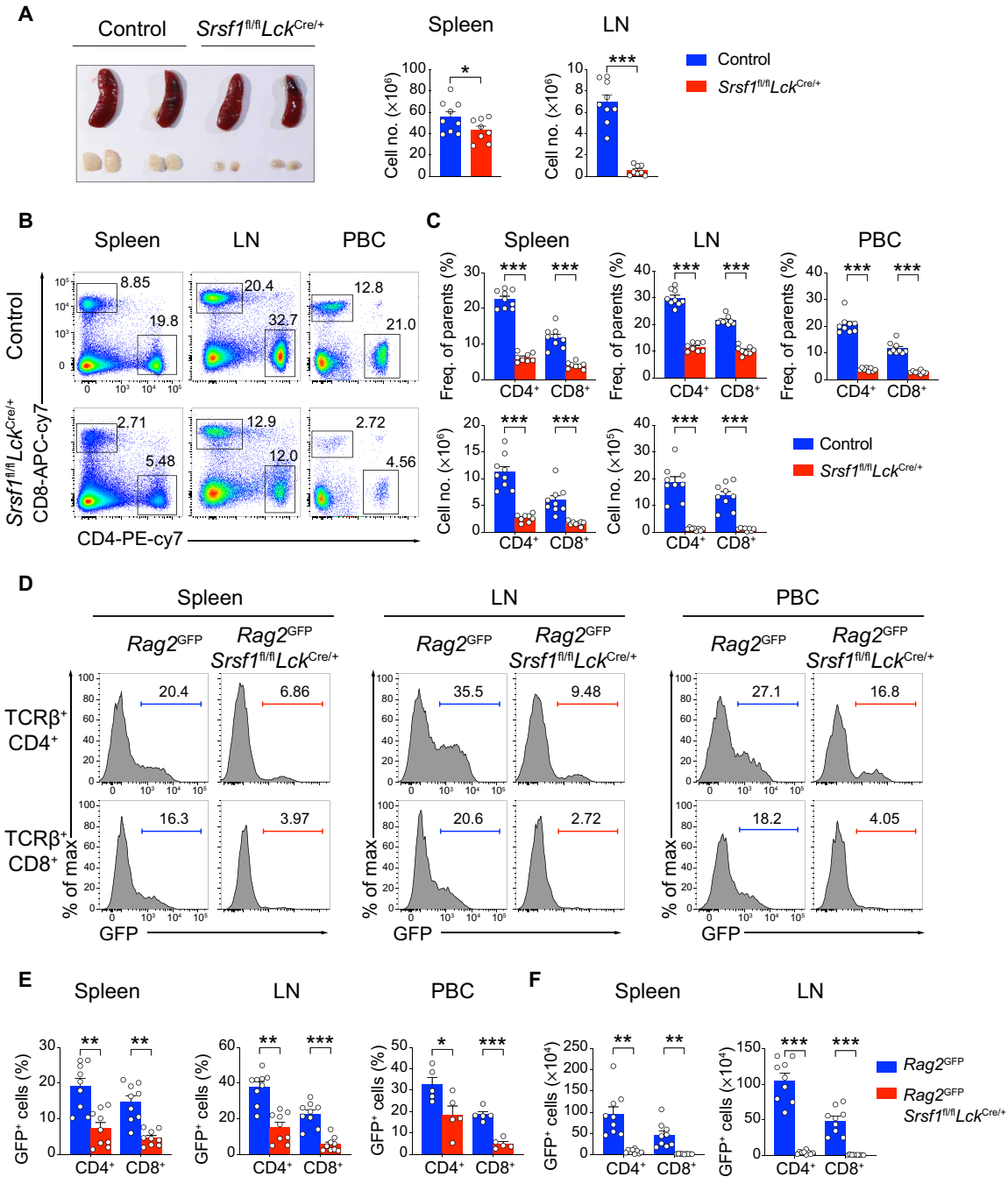

Fig. 2. SRSF1 deficiency impairs the peripheral T cell pool due to severe reduction of RTEs. (**A**) Images and cell numbers of spleens and LNs from control ($n = 9$) and *Srsf1*$^{fl/fl}$*Lck*$^{Cre/+}$ ($n = 8$) mice. Photo credit: Z. Qi, China Agricultural University. (**B**) Analysis of peripheral T cells. Representative pseudocolor plots show the CD4$^+$ and CD8$^+$ T cells in spleens, LNs, and PBCs. (**C**) Frequency and numbers of CD4$^+$ and CD8$^+$ T cells from indicated subsets in (B) are shown accordingly (control: $n = 9$; *Srsf1*$^{fl/fl}$*Lck*$^{Cre/+}$: $n = 8$). (**D**) Analysis of RTEs. TCRβ$^+$ CD4$^+$and CD8$^+$ T cells from spleen, LNs, and PBCs of *Rag2*^{GFP}*Srsf1*$^{fl/fl}$*Lck*$^{Cre/+}$ and littermate *Rag2*^{GFP} (as control) mice were measured by flow cytometry. Representative histograms show the percentages of GFP$^+$ cells from indicated populations. (**E** and **F**) Frequency (E) and numbers (F) of GFP$^+$CD4$^+$ and GFP$^+$CD8$^+$ T cells in spleen (left, $n = 9$) and LNs (middle, $n = 9$) or frequency (E) of GFP$^+$CD4$^+$ and GFP$^+$CD8$^+$ T cells in PBCs (right, $n = 5$) from mice with indicated genotype are shown accordingly. Cumulative data are means ± SEM. *$P < 0.05$, **$P < 0.01$, and ***$P < 0.001$ (Student's t test). Data are from at least three independent experiments.

TCRβ^{hi}CD69$^-$CD24$^-$ CD4$^+$ or CD8$^+$ SP thymocytes. The expression level of IL-7Rα was remarkably reduced in mature SP thymocytes from *Srsf1*$^{fl/fl}$*Lck*$^{Cre/+}$ mice (Fig. 3, E and F). Accordingly, the expression of proapoptotic genes *Bax* and *Bcl2l11* was notably up-regulated in SRSF1-deficient mature CD4$^+$ or CD8$^+$ SP thymocytes (Fig. 3G). These data thus demonstrated that SRSF1 deficiency resulted in defective proliferation, which is in accordance with the impaired IL-7Rα expression in mature SP thymocytes.

To further confirm the defects in thymocyte survival and proliferation, excluding the microenvironment factors, we performed

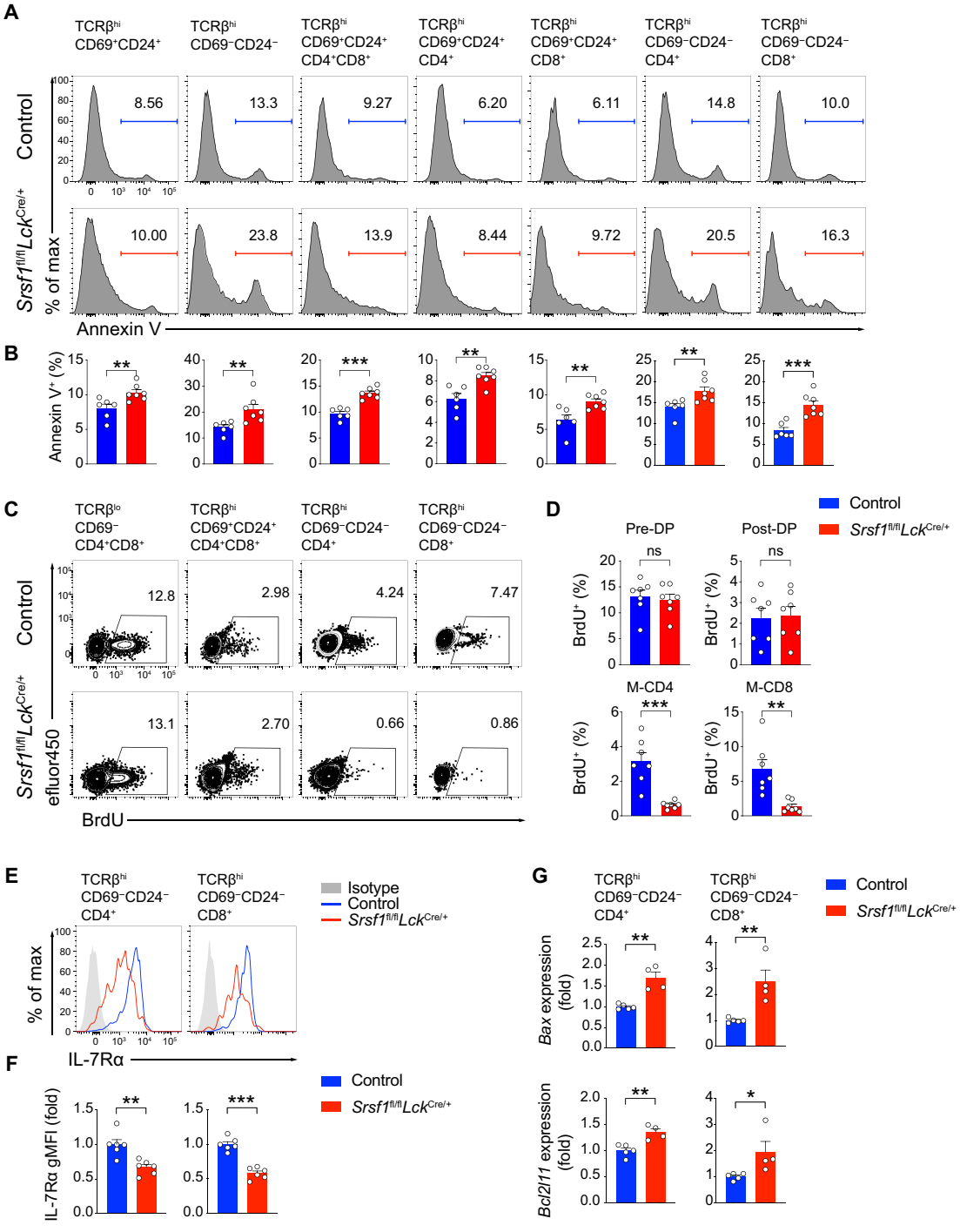

Fig. 3. SRSF1 is required for thymocyte proliferation and survival. (**A** and **B**) Apoptosis in postselection thymocyte subsets was analyzed with annexin V staining. Representative histograms (A) show the percentages of annexin V$^+$ cells in indicated subsets from control ($n = 6$) and *Srsf1*$^{fl/fl}$*Lck*$^{Cre/+}$ ($n = 7$) mice. Cumulative data on frequency of annexin V$^+$ cells are shown in (B). (**C** and **D**) BrdU incorporation was detected in TCRβ^{lo}CD69$^-$CD4$^+$CD8$^+$ DP cells (pre-DP), TCRβ^{hi}CD69$^+$CD24$^+$CD4$^+$CD8$^+$ DP cells (post-DP), mature TCRβ^{hi}CD69$^-$CD24$^-$CD4$^+$ SP (M-CD4), and mature TCRβ^{hi}CD69$^-$CD24$^-$CD8$^+$ SP (M-CD8) thymocytes, respectively. Representative contour plots (C) show BrdU$^+$ cells in indicated subsets from control (top row) and *Srsf1*$^{fl/fl}$*Lck*$^{Cre/+}$ mice (bottom row). Cumulative data on frequency of BrdU$^+$ cells are shown in (D) ($n = 7$ per group). (**E** and **F**) IL-7Rα expression on mature TCRβ^{hi}CD69$^-$CD24$^-$CD4$^+$ and TCRβ^{hi}CD69$^-$CD24$^-$CD8$^+$ SP thymocytes was detected from control and *Srsf1*$^{fl/fl}$*Lck*$^{Cre/+}$ mice ($n = 6$ per group) (E). Cumulative data on geometric mean fluorescence intensity (gMFI) are shown in (F). The geometric mean fluorescence intensity of IL-7Rα from control cells was set as 1, and its relative expression in cells from *Srsf1*$^{fl/fl}$*Lck*$^{Cre/+}$ mice was normalized accordingly. (**G**) qPCR validation of genes involved in apoptosis in mature CD4$^+$ and CD8$^+$ SP thymocytes from control ($n = 5$) and *Srsf1*$^{fl/fl}$*Lck*$^{Cre/+}$ ($n = 4$) mice. The relative expression of each transcript (after normalization to *Gapdh*) in control cells was set as 1 and that in cells from *Srsf1*$^{fl/fl}$*Lck*$^{Cre/+}$ mice was normalized accordingly. Cumulative data are means ± SEM. *$P < 0.05$, **$P < 0.01$, and ***$P < 0.001$ (Student's *t* test). All data are from at least three independent experiments.

thymocyte transfer assay in vivo as depicted in fig. S3A. Compared with the well-maintained wild-type (WT) donor cells in the hosts, those cells derived from SRSF1-deficient donor were substantially decreased on both days 3 and 7 after transfer (fig. S3, B and C). The transferred cells did not undergo proliferation on day 3, and the expansion of donor cells can be traced on day 7 after transfer (*28*). Therefore, the results on these two check time points strongly suggested that SRSF1 deletion resulted in inherent survival and proliferation defects in the thymocytes from *Srsf1*$^{fl/fl}$*Lck*$^{Cre/+}$ mice.

SRSF1 regulates T cell development in a cell-intrinsic manner

To determine whether the defects on thymocyte development in the absence of SRSF1 are caused in a cell-intrinsic manner, we generated bone marrow (BM) chimeric mice as the flowchart depicted in Fig. 4A, and the recipient mice were analyzed 10 weeks after reconstitution. Under the identical environment from recipients, *Srsf1*$^{fl/fl}$*Lck*$^{Cre/+}$ (CD45.2$^+$) BM-derived thymocytes phenocopied primary SRSF1-deficient mice, exhibiting an increase in the frequency of DP cells and a remarkable decrease in percentages of CD4$^+$ and CD8$^+$ SP cells (Fig. 4, B and C). Consistently, *Srsf1*$^{fl/fl}$*Lck*$^{Cre/+}$ donor-derived thymocytes in chimeric mice exhibited the same developmental defects observed in primary *Srsf1*$^{fl/fl}$*Lck*$^{Cre/+}$ mice (Fig. 4, D and E). *Srsf1*$^{fl/fl}$*Lck*$^{Cre/+}$ donor-derived mature CD4$^+$ and CD8$^+$ T cells in spleens, LNs, and PBCs were notably reduced (fig. S4, A and B). Thus, these data indicated that SRSF1 is intrinsically required for the late stage development of thymocytes.

Genome-wide analysis of SRSF1-binding genes in mouse thymocytes

To further explore the molecular mechanisms by which SRSF1 regulates thymocyte development, we performed irCLIP-seq (infrared crosslinking-immunoprecipitation and high-throughput sequencing) to profile SRSF1-binding events in thymocytes, and two independent replicates with a high correlation in read counts (Spearman = 0.84) were pooled together for the following analysis (fig. S5, A and B). We found that more than half of the SRSF1-RNA cross-link sites mapped to exonic sequences (Fig. 5A). Through calculating the distributions of SRSF1-binding peaks within 100 to 300 nucleotides (nt) upstream or downstream of the constitutive splice site, we observed that SRSF1 "preferentially" bound to exons and enriched between 0 and 100 nt of the 5′ and 3′ exonic sequences flanking the constitutive splice sites (Fig. 5B). SRSF1-binding peaks in mouse thymocytes were significantly enriched in GA-rich consensus motifs (Fig. 5C), which was consistent with the consensus deduced from the mouse embryo fibroblast CLIP-seq (*29*). To gain insight into the potential function of SRSF1, we performed Gene Ontology (GO) analysis of SRSF1-binding genes and found that they were significantly enriched in critical events related to thymocyte development including T cell differentiation, T cell proliferation, apoptotic signaling pathway, and type I interferon signaling pathway (Fig. 5, D and E). It is worth mentioning that apoptosis-related genes *Il7ra*, *Bax*, and *Bcl2l11* described in Fig. 3 (E to G) were directly bound by SRSF1. These data imply SRSF1 functions as a crucial regulator in the development of thymocytes.

SRSF1 deficiency globally alters the gene expression and splicing

To explore the underlying mechanism of SRSF1-regulated gene expression involved in the late stage of thymocyte development, we performed RNA sequencing (RNA-seq) in TCRβ^{hi} DP thymocytes, which is the unique developmental stage with effectively deactivated SRSF1 and initially exhibited the defects in thymocytes from *Srsf1*$^{fl/fl}$ *Lck*$^{Cre/+}$ mice. A total of 731 genes were down-regulated, and 485 genes were up-regulated in SRSF1-deficient cells (P value of <0.05, $|\log_2\text{FoldChange}| \geq 0.6$) (Fig. 6A). Among these up-regulated genes, the pathways related to T cell apoptotic process and negative regulation of cell cycle were significantly enriched, and the down-regulated genes were involved in T cell proliferation, T cell differentiation, T cell activation, and pathways related to response to interferon-α, interferon-beta, and interferon-gamma (Fig. 6B). We next performed gene set enrichment analysis (GSEA), which does not set a preset fold change threshold but interrogates the behavior of the whole gene set changes. The gene sets of interferon-α, interferon-β, and interferon-γ response were positively enriched in control cells (down-regulated in SRSF1-deficient cells) (Fig. 6C). By quantitative polymerase chain reaction (qPCR) validation, several down-regulated genes that are essential for T cell development, proliferation, or survival were further confirmed (Fig. 6, D and E). Among these genes, *Runx3*, *Myc*, *Foxo1*, *Il2rb*, and *Smad7* were directly bound by SRSF1 (Fig. 5E), whereas *Icos* and *Irf4* without SRSF1-binding site were regarded as indirectly down-regulated genes in SRSF1-deficient cells. By contrast, the expression of several T cell regulators involved in the late stage development of thymocytes was not changed, including *Bcl11b*, *Itk*, *Jun*, *Mcl1*, *Runx1*, *Ube2i*, and *Zap70*, reflecting the specificity of the alterations in mRNA abundance due to ablation of SRSF1 (fig. S6A). Moreover, a group of type I interferon–related genes including *Ifi27l2a*, *Ifit1*, *Il27ra*, *Irf7*, *Isg15*, *Oas3*, *Oasl2*, *Slfn1*, *Stat1*, and *Xaf1* were down-regulated in SRSF1-deficient TCRβ^{hi} DP thymocytes (Fig. 6, F and G). However, only *Il27ra*, *Irf7*, and *Stat1* gene loci have the SRSF1-binding sites (Fig. 5E), reflecting that most of them were regulated by SRSF1 via an indirect manner. Together, these results indicated that ablation of SRSF1 directly or indirectly alters the expression of hallmark genes involved in T cell development, proliferation, survival, and type I interferon response.

Given the biological function of SRSF1 in modulating RNA splicing, the inclusion-level differences of five different types of AS events between *Srsf1*$^{fl/fl}$*Lck*$^{Cre/+}$ and control groups were calculated using the rMATS computational tool (fig. S6B). A total of 2317 AS events were identified, and those included 1742 skipped exons (SEs), 155 retained introns (RIs), 159 mutually exclusive exons (MXEs), 119 alternative 5′ splice sites (A5SSs), and 142 alternative 3′ splice sites (A3SSs). The abolishment of SRSF1 was associated with more skip of SEs and A3SSs or A5SSs, more retention of introns, and use of MXEs (fig. S6B). To better gain mechanistic insight into the direct role of SRSF1 in mRNA splicing of thymocytes, we further interrogated the SRSF1 CLIP-seq data and inferred that SRSF1 directly regulated AS events from the binding of SRSF1 in the vicinity of the AS events. The proportion of SRSF1 that directly regulated AS events varied according to the types of AS events. The fraction of SRSF1-binding events in more skipped AS was comparable with those in more included AS events (fig. S6C), which suggested that the AS factor SRSF1 both repressed and activated AS in thymocytes. Together, our data identified that SRSF1 functions as a posttranscriptional regulator in thymocytes and specifically controls the mRNA abundance and AS in direct or indirect manners.

To address the direct targets that account for the T cell defects in SRSF1-deficient mice, we interrogated genes bound by SRSF1 and

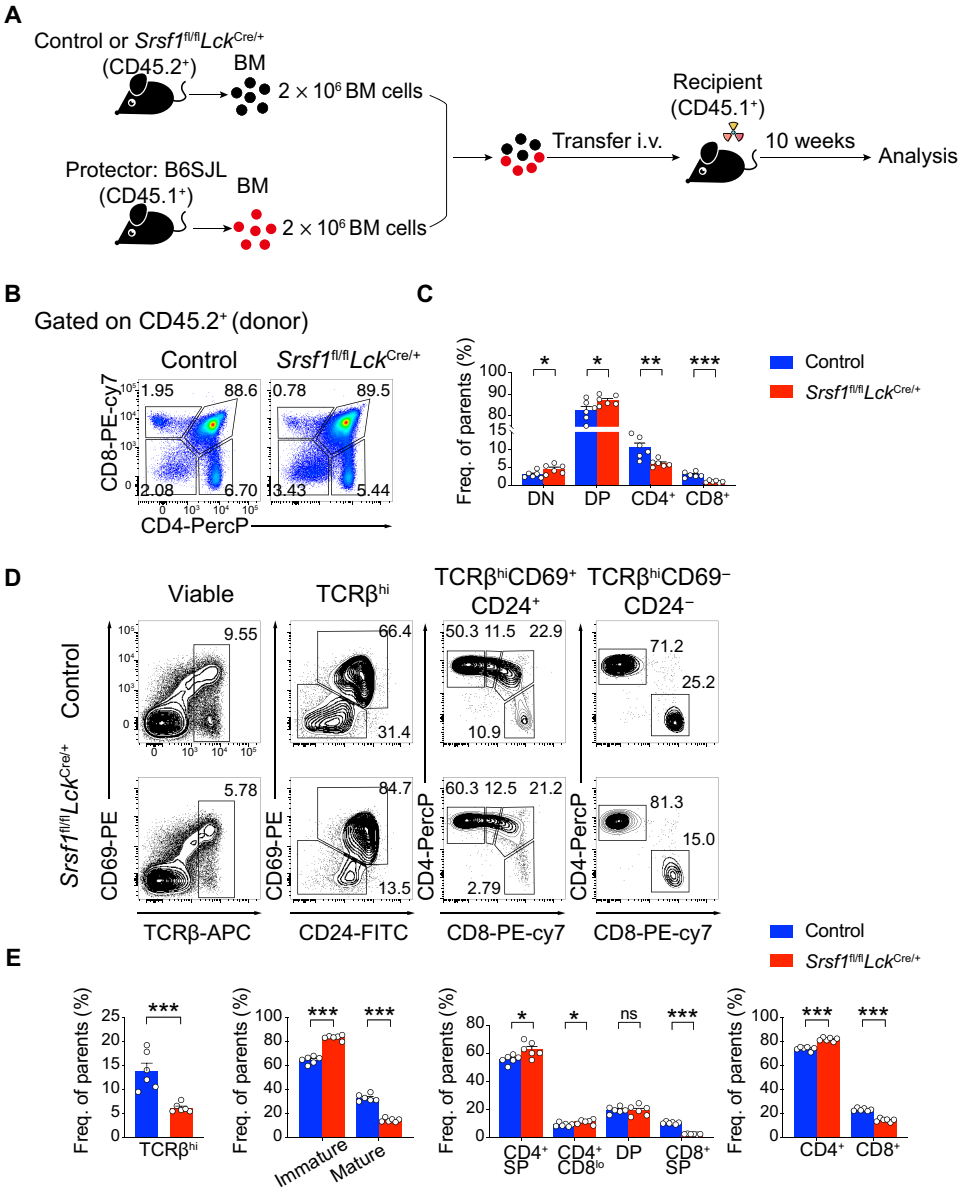

Fig. 4. SRSF1 regulates T cell development in a cell-intrinsic manner. (**A**) Flowchart of generation and analysis of BM chimeric mice. (**B**) Representative pseudocolor plot show the classic subsets of thymocytes with CD4 and CD8 staining from the chimeras generated with control and *Srsf1*$^{fl/fl}$*Lck*$^{Cre/+}$ donor (CD45.2$^+$) BM cells. (**C**) Frequency of indicated subsets as in (B) is shown accordingly ($n = 6$ per group). (**D**) Characterization of postselection thymocytes in chimeric mice. TCRβ^{hi} postselection thymocytes (CD45.2$^+$) derived from control and *Srsf1*$^{fl/fl}$*Lck*$^{Cre/+}$ mice in chimeras are shown by contour plot, and the gating strategies were consistent with those described in Fig. 1E. (**E**) Frequency of each subpopulation in (D) is statistically shown ($n = 6$ per group). Cumulative data are means ± SEM. *$P < 0.05$, **$P < 0.01$, and ***$P < 0.001$ (Student's *t* test). Data are from at least three independent experiments.

differentially expressed or alternatively spliced due to SRSF1 deficiency. Forty-six SRSF1 directly binding genes including *Irf7* and *Il27ra* were differentially spliced and down-regulated (Fig. 6, H and I), and both of them were known as essential regulators for the late stages of T cell development (*15*, *30*, *31*). *Irf7* also stands out as a common master regulator involved in response to type I interferons and interferon-gamma (*32*), both of which were impaired in SRSF1-deficient TCRβ^{hi} DP thymocytes (Fig. 6I). In addition, IL-27Rα functions as the receptor in IL-27 signaling, which is essential for the expression of Qa2 and IRF7 in the late stages of thymocyte development (*31*, *33*). Thus, the down-regulation and differentially alternative splicing of *Irf7* and *Il27ra* may account for the defective development of late thymocytes in *Srsf1*$^{fl/fl}$*Lck*$^{Cre/+}$ mice.

SRSF1 directly regulates splicing and expression of *Irf7* and *Il27ra*

We next investigated SRSF1-mediated regulation on the expression of *Irf7* and *Il27ra* via an integrated analysis of the RNA-seq and CLIP-seq data. A complex AS pattern in *Irf7* mRNA with increased inclusion of distal 3′ splicing site of exon 6 and retention of intron 5 was exhibited, and *Il27ra* mRNA showed reduced abundance and increased the ratio of exon 3 skipping in SRSF1-deficient cells

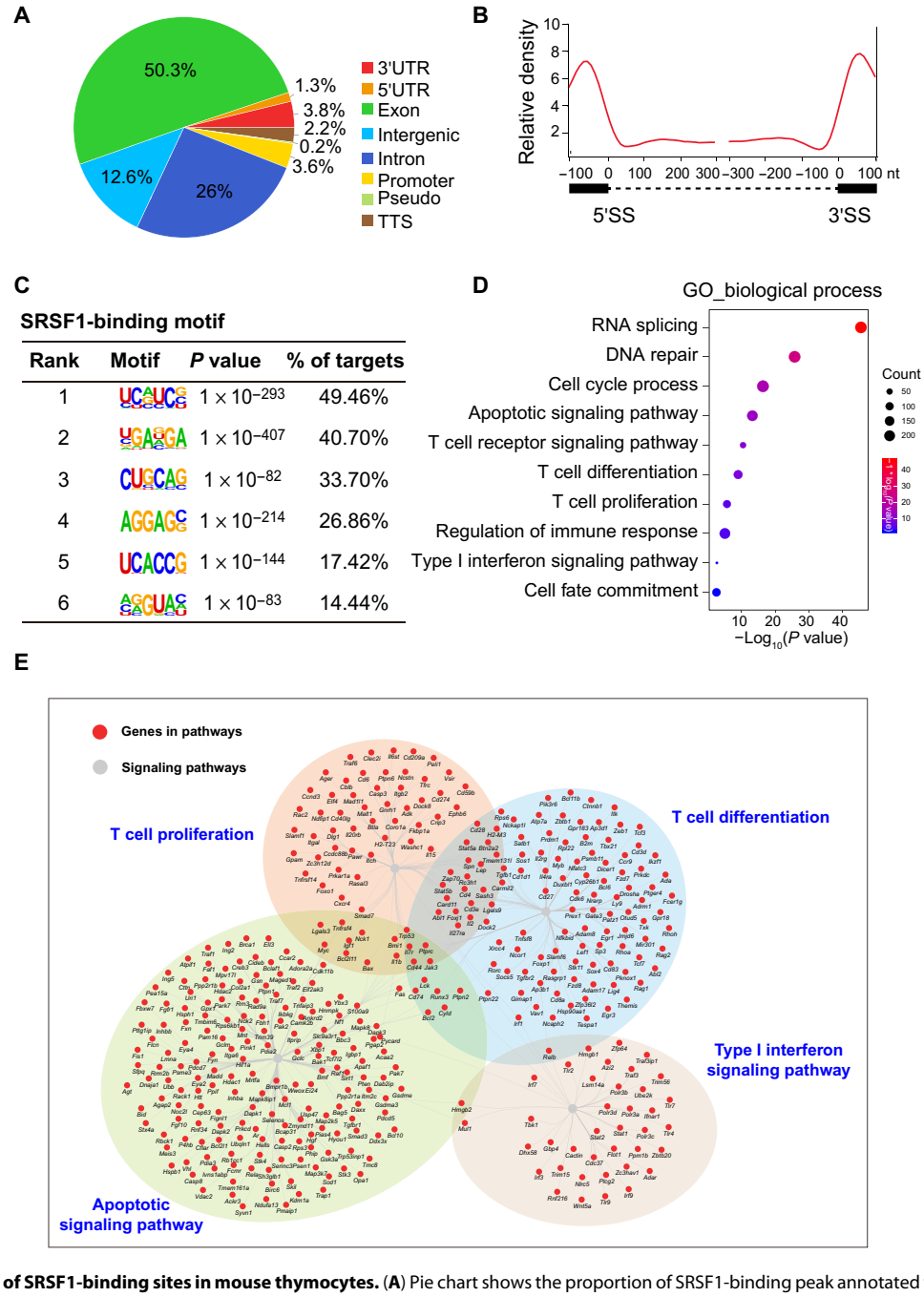

Fig. 5. Global landscape of SRSF1-binding sites in mouse thymocytes. (**A**) Pie chart shows the proportion of SRSF1-binding peak annotated to the 3′ or 5′ untranslated region (UTR), exon, intron, intergenic, promoter, pseudo, and transcriptional termination site (TTS), which were assessed by CLIP-seq (FDR < 0.05). (**B**) Schematic analysis exhibits the distribution of SRSF1-binding sites in the vicinity of the 5′ exon-intron and the 3′ intron-exon boundaries (300 nt upstream and 100 nt downstream of 3′SS; 100 nt upstream and 300 nt downstream of 5′SS). (**C**) Enriched SRSF1-binding motifs. The top six enriched motifs and their *P* values are shown. (**D**) GO enrichment map of SRSF1-binding genes. Overrepresentation analysis was used to determine the statistical significance of enrichments. (**E**) SRSF1-binding genes incorporated in (D) were analyzed by using Cytoscape. The association network shows the subgroups based on the function of involved genes.

(Fig. 7A). Contrastively, a series of key T cell genes were bound by SRSF1 without ectopic AS, including *Bcl11b*, *Mcl1*, *Ube2i*, and *Zap70*. There is no difference in the number of reads for mapping to exon-exon junctions (fig. S7A), which suggested the specificity of SRSF1-related mRNA splicing. Further, the ectopic splicing due to SRSF1 deletion was confirmed by semiquantitative reverse transcription PCR (RT-PCR). The normal spliced full-length transcripts of *Irf7* (the intron 5 was spliced out, and the proximal 3′ splicing site was used) and *Il27ra* (the exon 3 was included) were markedly reduced due to ablation of SRSF1 (Fig. 7B). Through sequence analysis, we found that the increased intron 5 retention in *Irf7* mRNA gives rise to the premature termination codon (PTC) (fig. S7B), which resulted in the quick degradation of this transcript in both nucleus and cytoplasm as previously reported (*34*). On the other aspect, the

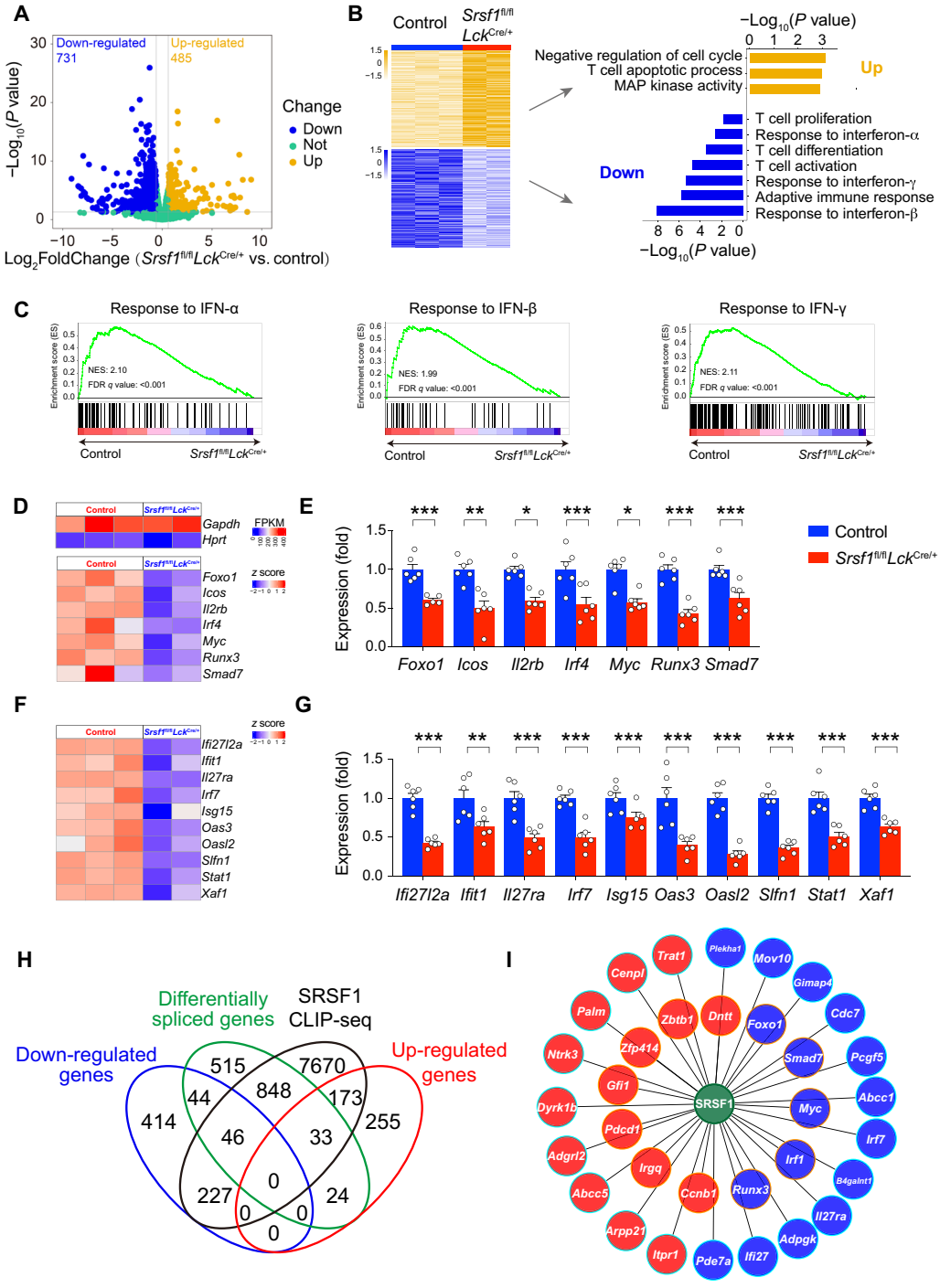

Fig. 6. SRSF1 deficiency altered the expression and splicing of transcripts in TCRβ^{hi} DP cells. (**A**) Volcano plots show the changes of mRNA abundance in RNA-seq of TCRβ^{hi} DP cells. DEGs were identified from *Srsf1*$^{fl/fl}$*Lck*$^{Cre/+}$ versus control (blue: down-regulated; yellow: up-regulated; green: unchanged). (**B**) Heatmap of significantly altered genes (left) and representative enriched GO terms (right). MAP, mitogen-activated protein. (**C**) GSEA was performed for interferon-α (IFN-α), interferon-β (IFN-β), and interferon-γ (IFN-γ) response pathways. NES, normalized enrichment score. (**D**) Heatmap shows the mRNA abundance of housekeeping genes (*Gapdh* and *Hprt*) and key T cell regulators. FPKM, fragments per kilobase million. (**E**) The expression of key T cell regulators was validated by qPCR in TCRβ^{hi} DP cells ($n \geq 5$ per group). The relative expression was normalized as described in Fig. 3G. (**F**) Heatmap shows the mRNA abundance of type I interferon response genes. (**G**) The expression of type I interferon response genes was validated by qPCR in TCRβ^{hi} DP cells ($n \geq 5$ per group). The relative expression was normalized as described above. (**H**) Venn diagram shows the correlation among DEGs, alternatively spliced genes, and SRSF1-binding genes. (**I**) SRSF1-centered regulatory network. Filled color represents the gene expression relationship with SRSF1 deficiency (red: up-regulation; blue: down-regulation). Border color represents the difference in AS with SRSF1 deficiency [ectopic splicing (blue) or not (orange)]. Solid line indicates the connected genes that were directly bound by SRSF1. Cumulative data are means ± SEM. *$P < 0.05$, **$P < 0.01$, and ***$P < 0.001$ (Student's *t* test). Data are from at least three independent experiments.

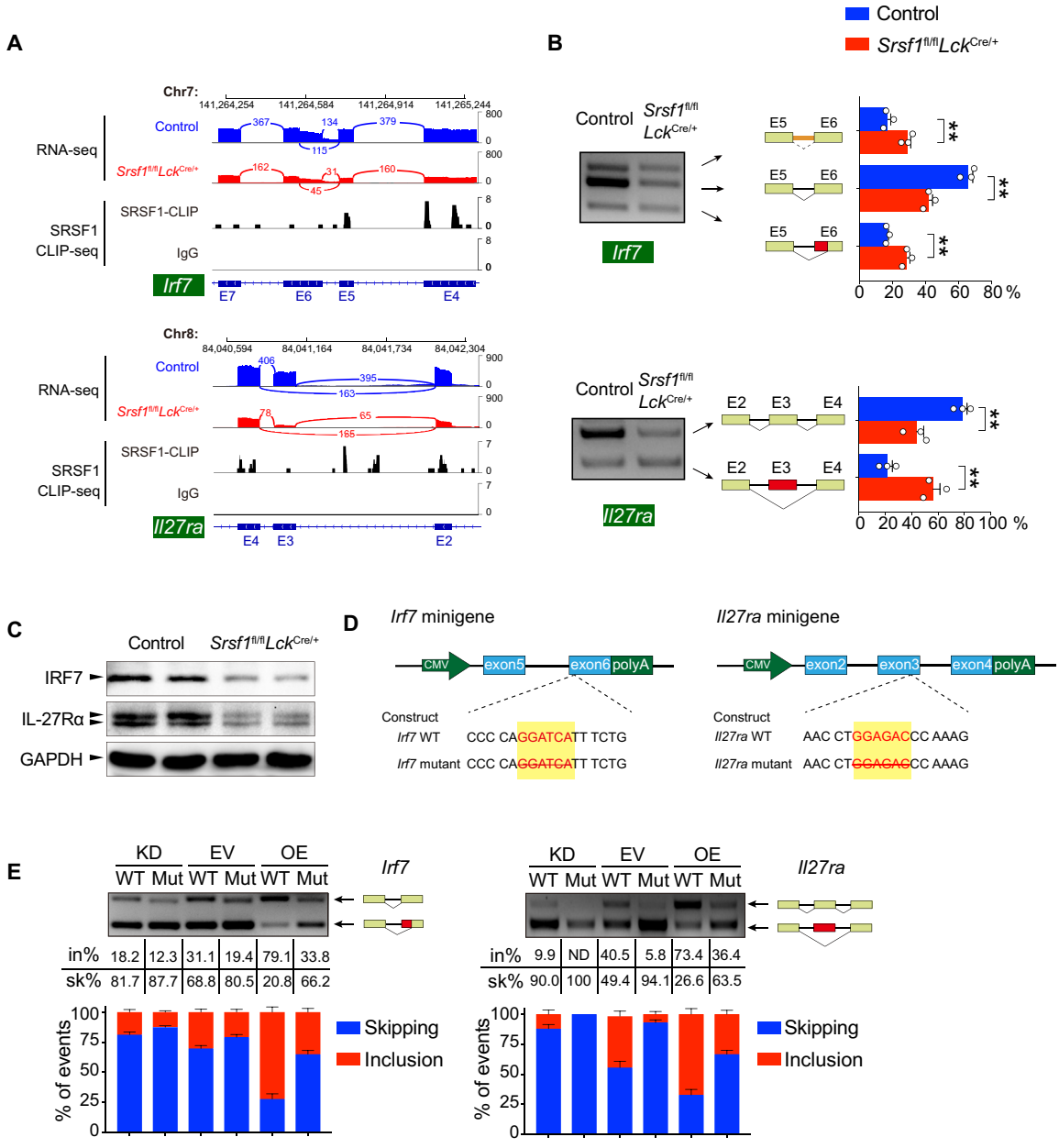

Fig. 7. SRSF1 directly regulates splicing and expression of *Irf7* and *Il27ra*. (**A**) Analysis of *Irf7* and *Il27ra* expression and exon-exon junctions. "Sashimi plots" show read coverage and exon-exon junctions (numbers on arches indicate junction reads), and the SRSF1-binding peaks of *Irf7* and *Il27ra* transcripts are shown. IgG, immunoglobulin G. (**B**) The ectopic splicing of *Irf7* and *Il27ra* in TCRβ^{hi} DP cells was analyzed by semiquantitative RT-PCR ($n = 3$ per group). The scheme and cumulative data on percentage of the indicated fragment are shown accordingly. (**C**) The protein level of IRF7 and IL-27Rα was determined in DP thymocytes by Western blot. GAPDH, glyceraldehyde-3-phosphate dehydrogenase. (**D**) Graphical representation of *Irf7* and *Il27ra* minigenes. The potential SRSF1-binding sites are marked in red characters, and the specific deletion mutations are indicated with a strikeout. (**E**) Analysis of the splicing of *Irf7* and *Il27ra* minigenes by semiquantitative RT-PCR. The constructs with (WT) or without (Mut) SRSF1-binding site were applied for splicing assay under the indicated conditions (KD: SRSF1 knockdown; EV: empty vector; OE: SRSF1 overexpression). The percentages of inclusion (in%; red) and skipping (sk%; blue) within exon 6 of *Irf7* or exon 3 of *Il27ra* transcripts are presented, respectively. Data are means ± SEM. $^{**}P < 0.01$ (Student's *t* test). Data are representative of at least three independent experiments. CMV, cytomegalovirus; ND, not determined.

increased usage of the distal 3′ splicing site of exon 6 with the loss of 96 base pairs (bp) compromised the abundance of full-length *Irf7* transcript (Fig. 7B and fig. S7B). Meanwhile, the skipping of exon 3 in *Il27ra* mRNA caused a frameshift and introduced PTC (fig. S7C), which subsequently resulted in nonsense-mediated mRNA decay (NMD) (*35*). Western blot analysis further confirmed that AS events described as above led to severe reduction of IRF7 and IL-27Rα proteins in SRSF1-deficient cells (Fig. 7C).

To verify the role of SRSF1 via directly binding in regulating AS of *Irf7* and *Il27ra* RNA, we constructed minigene vectors containing the mouse genomic DNA fragment with/without SRSF1-binding motifs of *Irf7* exon 6 and *Il27ra* exon 3, respectively (Fig. 7D).

Splicing assay in vitro was carried out in 293T cells transfected by minigene vectors together with KD/EV/OE plasmid of SRSF1. In accordance with the endogenous splicing pattern, the proportion of inclusion in *Irf7* and *Il27ra* minigene was increased in the presence of SRSF1 compared with empty vectors, whereas SRSF1 knockdown markedly inhibited the inclusion of the relative exons (Fig. 7E). The deletion of SRSF1-binding site in exon 6 of *Irf7* caused the switching of SRSF1-dependent inclusion to skipping of a part of exon 6. Similarly, the deletion of SRSF1-binding site in exon 3 of *Il27ra* caused the switching of SRSF1-dependent inclusion to skipping of exon 3 (Fig. 7E). These data thus suggested that SRSF1 controls the expression levels of IRF7 and IL-27Rα by directly binding and modulating their transcript splicing.

Enforced expression of IRF7 could rectify the defects in the maturation of SRSF1-deficient thymocytes

IRF7 was previously reported as a master regulator in response to type I interferon, which serves as the downstream target of IL-27 signaling during the late stage of T cell development (*31*). Thus, we next attempted to explore whether enforced expression of IRF7 could rectify the defects in the maturation of late thymocytes caused by SRSF1 deficiency. To achieve this goal, lineage-negative BM cells of chimeric mice were constructed and analyzed as described in the flowchart (fig. S8A). We verified *Srsf1* expression and confirmed that *Irf7* was successfully overexpressed in donor-derived cells with indicated genotypes (fig. S8, B and C). Analysis of CD45.2$^+$GFP$^+$TCRβ^{hi} postselection thymocytes showed that the reduction of mature (TCRβ^{hi}CD69$^-$CD24$^-$) thymocytes was substantially restored by forced expression of IRF7 compared with those derived from Control-*MigR1* or *Srsf1*$^{fl/fl}$*Lck*$^{Cre/+}$-*MigR1* donors (top row in Fig. 8, A and B). We further analyzed the reconstitution of CD4$^+$ and CD8$^+$ T cells in CD45.2$^+$GFP$^+$ immature and mature thymocyte subsets; the frequency of both immature and mature CD8$^+$ SP cells was rescued with the forced expression of IRF7 (second and bottom rows in Fig. 8, A and B). In addition, ectopic expression of IRF7 also rectified the proportions of CD4$^+$ and CD8$^+$ T cells in SRSF1-deficient CD45.2$^+$GFP$^+$TCRβ^{hi} postselection thymocytes (Fig. 8C). Furthermore, IRF7 overexpression also elevated the cell proportion of CD69$^-$Qa2$^+$ cells in both CD45.2$^+$GFP$^+$TCRβ^{hi} CD4$^+$ and CD8$^+$ SP thymocytes (Fig. 8, D and E). Meanwhile, the mature CD4$^+$ or CD8$^+$ T cells in spleen and LNs were significantly increased in IRF7 overexpressed cells compared with those from *MigR1*-transduced SRSF1-deficient controls but were still not comparable with *MigR1*-transduced WT controls (fig. S8, D and E). Besides, we also confirmed that ectopic overexpression of IRF7 could largely restore the expression levels of type I interferon–related genes in CD45.2$^+$GFP$^+$TCRβ^{hi} DP thymocytes (Fig. 8F). Collectively, these data demonstrated that enforced expression of IRF7 substantially restores defects on the maturation of SRSF1-deficient thymocytes and rectifies the expression of a set of type I interferon–related genes corresponding to T cell late stage development.

In summary, conditional deletion of SRSF1 in DP thymocytes leads to a substantial reduction of TCRβ^{hi} population and a severe blockade of the transition of TCRβ^{hi}CD24$^+$CD69$^+$ immature thymocytes to TCRβ^{hi}CD24$^-$CD69$^-$ mature thymocytes. Meanwhile, loss of SRSF1 leads to the down-regulated expression of Qa2 in both mature CD4 SP and CD8 SP thymocytes. As a result, the RTEs were markedly diminished corresponding to the impaired periphery T cell pool in SRSF1-deficient mice. SRSF1 intrinsically promotes the proliferation and inhibits apoptosis of those thymocytes by modulating a series of genes, which are essential for T cell intrathymic maturation. Meanwhile, SRSF1 regulates the AS of type I interferon pathway–related factors IRF7 and IL-27Rα to safeguard the late stage of thymocyte development in a cell-intrinsic manner (Fig. 9).

DISCUSSION

Elucidation of the mechanism by T cell intrathymic maturation has always been one of the major quests in developmental immunology. Although the transcriptional regulation programs of T cell development have been extensively investigated, it remains largely unknown about the posttranscriptional regulation mechanisms that control the late stage of thymocyte fate. The impact of RNA binding proteins (RBPs) that have the potential to integrate multiple aspects of gene expression provides emerging directions in deciphering the complicated regulatory layers of T cell development. SRSF1 as a pivotal RBP has well-documented roles that functions as posttranscriptional regulator for mRNA splicing and translation, which are involved in basic physiological processes and multiple cancer genesis (*36*, *37*). A recent study reported that conditional targeting of SRSF1 with distal *Lck*-Cre resulted in aberrant mature T cell activation and systemic autoimmunity due to limitation on expression of the mTOR repressor PTEN (*17*). However, there are no obvious defects in T cell development in their SRSF1-deficient mice owing to the effective deletion that occurs in thymocytes at a very late stage (*38*).

In this study, we demonstrate the crucial roles of SRSF1 in promoting late thymocyte development. SRSF1 plays a critical role in promoting the development of late thymocyte and maintaining peripheral T cell pool. On one hand, SRSF1 inhibits apoptosis of postselection thymocytes and upholds the mature thymocyte proliferation by modulating a series of genes, which are essential for T cell expansion and survival. On the other hand, SRSF1 regulates the expression of IRF7 and IL-27Rα via AS in response to type I interferon signal pathway to safeguard the down-regulation of CD69 and CD24 and the up-regulation of Qa2 for terminal maturation before egress. These findings illustrate that SRSF1 has a previously unknown role in the late stage of T cell development by posttranscriptional regulatory mechanisms.

All thymocytes that express TCRs are subjected to a selection process at the DP stage and are triggered to progress to the differentiation and proliferation of CD4 SP and CD8 SP stage or undergo apoptotic death (*39*, *40*). Loss of SRSF1 in the TCRβ^{hi} DP stage leads to compromised proliferation of TCRβ^{hi}CD69$^-$CD24$^-$ mature SP thymocytes. Meanwhile, the elevated apoptosis in SRSF1-deficient thymocytes was exhibited throughout the developmental process from the TCRβ^{hi} DP to TCRβ^{hi}CD24$^-$CD69$^-$ mature SP stage. Consistent with the previous studies that the proliferation and survival of thymocytes at late stage are associated with IL-7 signaling depending on the intrinsic expression of IL-7Rα (*26*, *41*), we found substantial down-regulation of IL-7Rα in SRSF1-deficient TCRβ^{hi} CD24$^-$CD69$^-$ mature subsets. Correspondingly, the abundance of *Bax* and *Bcl2l11*, both of which function as proapoptotic factors in thymocytes (*42*, *43*), was up-regulated in mature thymocytes due to SRSF1 deletion. These findings thus suggested that SRSF1 is essential for the differentiation, proliferation, and survival of late thymocytes.

The analysis of CLIP-seq in thymocytes showed that a large number of genes were directly bound by SRSF1, which are involved in T cell differentiation, proliferation, survival, and especially in

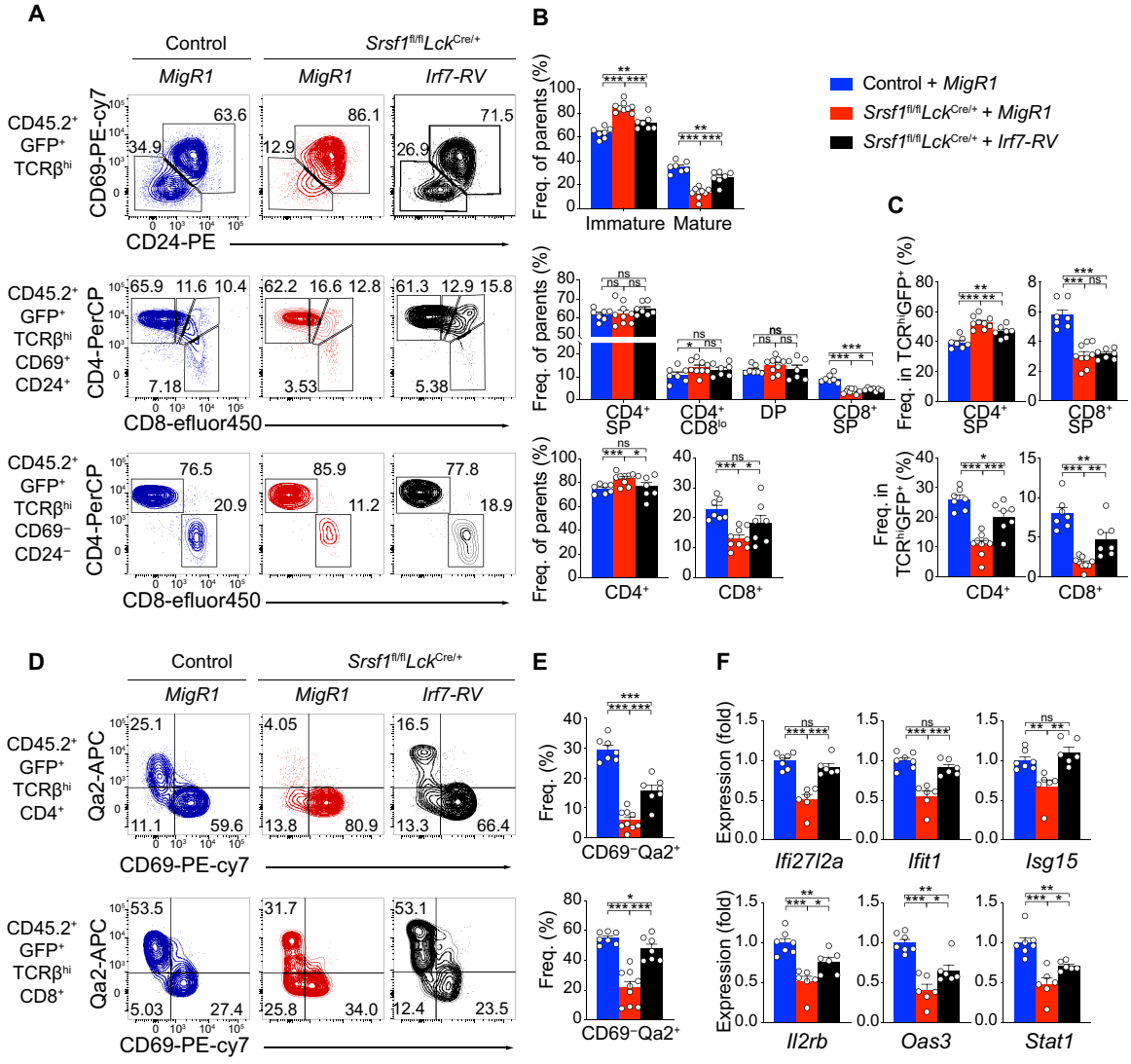

Fig. 8. Forced expression of IRF7 substantially rectified the terminal maturation of SRSF1-deficient thymocytes. (**A**) Analysis of late thymocyte development in chimeras with forced expression of IRF7. Donor-derived CD45.2$^+$GFP$^+$TCRβ^{hi} cells were fractionated into CD69$^+$CD24$^+$ immature and CD69$^-$CD24$^-$ mature subsets (top row). The immature subset (second row) and the mature subset (bottom row) were further subdivided by CD4 and CD8. (**B**) Frequency of indicated subsets in (A) is shown accordingly (control-*MigR1*: $n = 7$; *Srsf1*$^{fl/fl}$*Lck*$^{Cre/+}$-*MigR1*: $n = 9$; *Srsf1*$^{fl/fl}$*Lck*$^{Cre/+}$-*Irf7-RV*: $n = 7$). (**C**) Proportion of immature (top) and mature (bottom) CD4$^+$ and CD8$^+$ SP cells in donor-derived postselection thymocytes (CD45.2$^+$GFP$^+$TCRβ^{hi}). The percentage of each indicated population is shown. (**D**) Representative contour plots show the expression of CD69 and Qa2 in donor-derived CD45.2$^+$GFP$^+$TCRβ^{hi} CD4$^+$ and CD8$^+$ SP thymocytes (control-*MigR1*: $n = 7$; *Srsf1*$^{fl/fl}$*Lck*$^{Cre/+}$-*MigR1*: $n = 9$; *Srsf1*$^{fl/fl}$*Lck*$^{Cre/+}$-*Irf7-RV*: $n = 7$). (**E**) Frequency of CD69$^-$Qa2$^+$ T cells from indicated subsets is shown accordingly (control-*MigR1*: $n = 7$; *Srsf1*$^{fl/fl}$*Lck*$^{Cre/+}$-*MigR1*: $n = 9$; *Srsf1*$^{fl/fl}$*Lck*$^{Cre/+}$-*Irf7-RV*: $n = 7$). (**F**) Expression of type I interferon–regulated genes in CD45.2$^+$GFP$^+$TCRβ^{hi} DP thymocytes sorted from BM chimeras as in (A) (control-*MigR1*: $n = 7$; *Srsf1*$^{fl/fl}$*Lck*$^{Cre/+}$-*MigR1*: $n = 6$; *Srsf1*$^{fl/fl}$*Lck*$^{Cre/+}$-*Irf7-RV*: $n = 6$). The relative expression of each target transcript was normalized as described in Fig. 3G. Data are means ± SEM. *$P < 0.05$, **$P < 0.01$, and ***$P < 0.001$ (Student's *t* test). Data are representative from three independent experiments.

type I interferon signaling pathway. Our RNA-seq data further indicated that SRSF1 deficiency resulted in global changes of mRNA abundance and ectopic splicing of pre-mRNA. We found that ~70% of those differentially expressed genes (DEGs) have SRSF1-RNA interactions and that approximately half of the ectopic splicing events have SRSF1 binding in the vicinity of corresponding transcripts. By combining RNA-seq and CLIP-seq analyses, we found that *Foxo1*, *Myc*, *Runx3*, and *Smad7* as direct binding targets of SRSF1 were notably down-regulated in TCRβ^{hi} DP thymocytes, whereas the reduced expression of *Icos*, *Il2rb*, and *Irf4* was indirectly regulated by SRSF1. These genes described above were tightly correlated with thymocyte proliferation and survival (*44*–*48*). Foxo1 links T cell homing and survival by regulating L-selectin, CCR7, and IL-7 receptor (*49*); the lack of Smad7 blunts T cell proliferation (*45*); CD122 (encoded by *Il2rb*) is essential for IL-2– or IL-15–driven T cell proliferation (*50*); Myc is a well-known regulator for T cell proliferation and survival (*51*). Thus, the reduced abundance of these genes accounts for the severe reduction of immature and mature SP thymocytes in the absence of SRSF1.

The impairment of type I interferon treatment on T cell development was previously reported (*30*), and there is an increasing appreciation that type I interferon signaling sustains homeostasis of

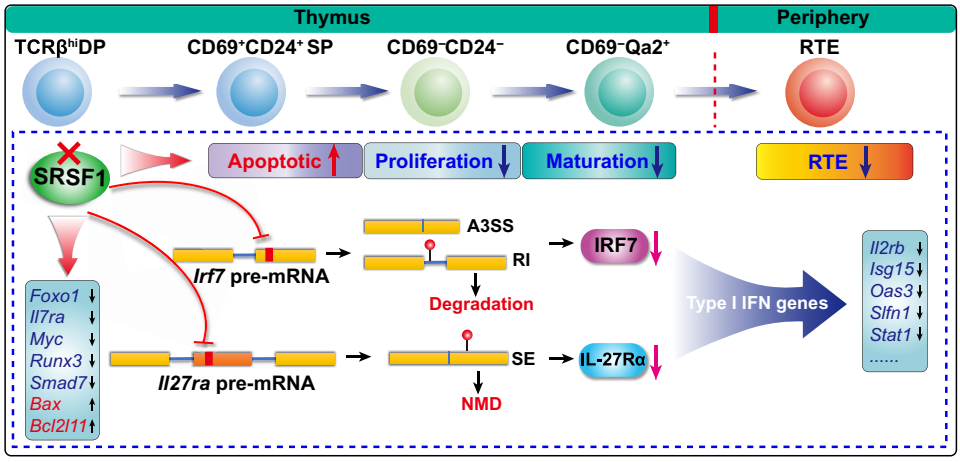

Fig. 9. A schematic illustration of molecular mechanisms by which SRSF1 regulates the late stage of thymocyte development. The continuous processes of post-selection thymocyte maturation before egression to periphery are shown on the top of the diagram. The red cross mark represents the deletion of SRSF1 in TCRβ^{hi} DP thymocytes. The accelerated apoptosis, impaired proliferation, blockade of terminal maturation, and notably diminished RTEs in SRSF1-deficient mice are exhibited with arrows (up: increased; down: decreased) following "apoptotic," "proliferation," "maturation," and "RTE." Mechanically, SRSF1 directly binds and regulates the splicing of *Irf7* and *Il27ra* pre-mRNA. In SRSF1-deficient thymocytes, the aberrant splicing of *Irf7* and *Il27ra* mRNAs results in the accelerated degradation of *Irf7* transcripts and NMD of *Il27ra* transcripts, respectively. The protein levels of IRF7 and IL-27Rα were severely decreased (indicate with the magenta arrows), which compromised the expression of the type I interferon–related genes. In addition, SRSF1 deletion also perturbs the expression of *Foxo1*, *Il7ra*, *Myc*, *Runx3*, *Smad7*, *Bax*, and *Bcl2l11*, contributing to the aberrant apoptosis and proliferation of thymocytes. The black arrows following genes in the boxes indicate the down-regulated expression or up-regulated expression, respectively. The little red balls in the isoforms resulted from ectopic splicing show the generation of PTC.

other hematopoietic lineages (*32*). Type I interferon signaling also plays cell-intrinsic roles in promoting T cell reconstruction in mixed BM chimeras (*52*). A recent study found that the expression of Qa2 in mature SP thymocytes was strongly dependent on type I interferon signaling (*15*). In this study, we observed that SRSF1-binding genes are strongly associated with the type I interferon signaling pathway, and loss of SRSF1 resulted in the marked down-regulation of a group of type I interferon–related genes. In particular, SRSF1 directly binds the transcripts of *Il27ra* and *Irf7* and regulates their expression via controlling AS. As the mediator of type I interferon signaling, IRF7 is constitutively expressed in thymocytes (*53*, *54*), which plays essential roles for thymic epithelial cell development and maintenance of the intact thymic architecture in responses to interferons (*55*). Our results suggested that SRSF1 regulated the expression of *Irf7* in a direct manner by facilitating the use of proximal 3′ splicing site of exon 6 and the splicing out of intron 5, which synthetically resulted in a deduction of IRF7 at protein level. Forcing expression of IRF7 not only restored the expression of type I interferon–related genes but also rectified the blocking phenotype in the transition from TCRβ^{hi}CD24^{+}CD69^{+} immature to TCRβ^{hi}CD69^{-}CD24^{-} mature SP thymocytes with elevated expression level of Qa2 in SRSF1-deficient thymocytes. Thus, as a bona fide target of SRSF1, IRF7 plays pivotal roles via modulating type I interferon–related genes in choreographing thymocyte terminal maturation.

The IL-27 signaling transduced by the receptor complex composed of the cytokine receptor IL-27Rα and GP130 is also indispensable for maintaining the expression of IRF7 and Qa2 during thymocyte maturation (*31*). Here, we found that SRSF1 deletion promoted the skipping of *Il27ra* exon 3 and consequently led to a frameshift and PTC generation in pre-mRNA, which would be eliminated by a surveillance mechanism termed as NMD (*35*). Together, the low abundance of IL-27Rα in SRSF1-deficient thymocytes would attenuate the strength of the IL-27 signaling response, which also contributed to the phenotype of reduced mature SP thymocytes.

In summary, the present study has provided a pivotal insight into the SRSF1-dependent posttranscriptional regulations governing the late stage of thymocyte development and sustaining the peripheral T cell pool. Our results reveal previously unknown roles of SRSF1 in the control of regulatory programs for late thymocytes in proliferation and apoptosis and in response to type I interferon signaling for terminal maturation. Further investigations of the mechanisms by which direct targets downstream of IRF7 and type I interferon signal contribute to the late stage of thymocyte development will be important to understand how they precisely modulate thymocyte maturation.

MATERIALS AND METHODS

Study design

SRSF1 is a pivotal splicing regulator involved in AS, mRNA decay, and translation to regulate cell fate. The aim of this study was to characterize the role of SRSF1 in the late stage of thymocyte development. Lck cre transgenic mice and *Srsf1*$^{fl/fl}$ mice on C57BL/6J background were bred together to generate the mice model with conditional deletion of SRSF1 in thymocytes beyond the ISP stage. To avoid the potential effects caused by Lck Cre transgene from homozygous mice, we performed all the experiments with *Srsf1*$^{fl/fl}$*Lck*$^{Cre/+}$ mice (Lck Cre transgene is hemizygous) in comparison with mice without Lck Cre transgene as their littermate controls. All experiments were repeated at least three times with the exception of BM chimeric models, which were repeated two times. Multiple cell and molecular biological approaches were applied for the phenotype and mechanism assays, including cell isolation, flow cytometry, cell

sorting, cell proliferation, apoptosis, qPCR, RNA-seq, and CLIP-seq. Specific information about sample numbers and data analysis is described in the figure legends.

Animals

Srsf1$^{fl/fl}$ mice were provided by X.-D. Fu (University of California, San Diego). RAG2p-GFP transgenic mice were provided by R. Jin (NHC Key Laboratory of Medical Immunology, Peking University). *Lck*-Cre (JAX: 006889), C57BL/6, and B6.SJL (CD45.1$^+$) mice were obtained from the Jackson laboratory. Six- to 10-week-old mice were used for the overall experiments in this study. All mice were bred and housed under specific pathogen–free conditions under controlled temperature (22° ± 1°C) and exposed to a constant 12-hour light-dark cycle in the animal facilities at China Agricultural University. All experiments were conducted in accordance with the guidelines and with the approval of the Institutional Animal Care and Use Committee of China Agricultural University.

Flow cytometry

Single-cell suspensions were isolated and prepared from thymus, spleen, LNs, and PBCs. Cells were stained with indicated antibodies. Fluorochrome-conjugated antibodies against CD24 (M1/69), CD69 (H1.2F3), CD4 (RM4-5), TCRβ (H57-597), CD8a (53-6.7), CD44 (IM7), CD25 (PC61.5), CD3e (145-2C11), Gr.1 (RB6-8C5), B220 (RA3-6B2), TER119 (TER-119), CD11b (M1/70), CD11c (N418), CD49b (DX5), TCRγδ (GL-3), CCR7 (4B12), CD62L (MEL-14), CD45.2 (104), CD45.1 (A20), and annexin V (BMS306PE) were from eBioscience. Streptavidin (554063) was from BD Biosciences. Qa2 (6951-11-9-9) antibody was from BioLegend. S1P1/EDG-1 (713412) antibody was from R&D company. SRSF1 antibody (sc-33652) was from Santa Cruz Biotechnology. For the intracellular staining, cells were first stained by surface antibodies and then fixed and permeabilized with a Foxp3 staining buffer set (catalog no. 00-5523-00, eBioscience) according to the manufacturer's instructions. Subsequently, the permeabilized cells were stained by indicated antibodies diluted in permeabilization buffer. Data were acquired on a FACSVerse or an LSRFortessa (BD Biosciences) and analyzed with FlowJo software (version 10.4.0, Tree Star Inc.). For cell sorting, single-cell suspensions from control or *Srsf1*$^{fl/fl}$*Lck*$^{Cre/+}$ mice were surface-stained with indicated antibodies and sorted on a FACSAria II (BD Biosciences).

Gene expression analysis

Total RNA was extracted from sorted cells using the RNeasy Mini Kit (catalog no. 74106, Qiagen), following the manufacturer's instructions. The first-strand complementary DNA (cDNA) was synthesized using the FastQuant RT Kit (catalog no. KR106-02, Tiangen). Relative gene expression levels were analyzed by quantitative RT-PCR with the SYBR Green Master Mix (catalog no. FP205-02, Tiangen) using the CFX96 Connect Real-Time System (Bio-Rad). The primers are listed in table S1. *Gapdh* was used to normalize the relative expression of indicated genes, and the method of $2^{-\Delta CT}$ was used to calculate the expression levels of target mRNAs.

Semiquantitative PCR was carried out with primers amplifying endogenous transcripts (listed in table S1). The PCR products were analyzed on 2% agarose gels, and the percentage of each band was quantified with Image Lab 5.1 (Bio-Rad) software. The ratio among various isoforms was normalized to the total amount to calculate the relative abundance.

Proliferation and apoptosis analysis

For thymocyte proliferation assay by BrdU incorporation, the mice with indicated genotype were injected intraperitoneally with BrdU at the dosage of 100 mg/kg of body weight and analyzed 16 hours after injection. Cells were surface-stained, and then intracellular staining of BrdU was carried out using an FITC or APC BrdU Flow kit (catalog no. 559619 or 552598, BD Biosciences) following the manufacturer's instruction. For detection of thymocyte apoptosis, cells were stained with indicated surface antibodies and then stained with anti–annexin V and 7-AAD using the PE annexin V Apoptosis Detection Kit (catalog no. 559763, BD Biosciences) following the manufacturer's instruction.

Tracing cell survival in vivo

Thymocytes from control or *Srsf1*$^{fl/fl}$*Lck*$^{Cre/+}$ (CD45.2$^+$) mice were isolated as donors, and the thymocytes from WT mice on identical genetic background were used as competitors (CD45.1$^+$CD45.2$^+$). Cells from control or *Srsf1*$^{fl/fl}$*Lck*$^{Cre/+}$ mice were mixed with WT competitors at a 1:1 ratio, respectively, based on the number of CD4 SP T cells. Subsequently, 2×10^6 mixed cells were transferred via tail vein injection into each B6.SJL (CD45.1$^+$) recipient, which were irradiated half-lethally by a dose of 5 grays (Gy). On days 3 and 7 after cell transfer, the recipients were euthanized, and the proportion of T cells from blood, spleens, and LNs was analyzed to examine the contributions of donor cells.

Immunoblot analysis

To analyze IRF7 and IL-27Rα expression in CD4$^+$CD8$^+$ DP cells, the cell lysates were prepared, then separated by 10% SDS–polyacrylamide gel electrophoresis (PAGE), and transferred to a polyvinylidene difluoride membrane (catalog no. IPVH00010, Merck Millipore). IRF7 and IL-27Rα were detected with rabbit monoclonal antibodies from Abcam (anti-IRF7, ab238137; anti–IL-27Rα, ab220359). Visualization of anti-IRF7 and anti–IL-27Rα was carried out with a horseradish peroxidase–conjugated goat anti-rabbit immunoglobulin G (ZB-2301, ZSGB-BIO), respectively.

Minigene reporter assay

The WT *Il27ra* minigene was constructed by inserting an additional 1526 bp from exon 2 (corresponding to chr8: 84042202-84040677, mm10) into pcDNA3.1 vector between the Bam HI and Xba I sites. The WT *Irf7* minigene was constructed by inserting an additional 312 bp from exon 5 (corresponding to chr7: 141264487-141264798, mm10) into pcDNA3.1 vector between the Bam HI and Eco RI sites. The plasmids containing the mutant-binding site of SRSF1 were cloned with appropriate primers adjacent to the binding site using the site-directed mutagenesis approach.

To generate the expression plasmid for SRSF1, the CDS region of *Srsf1* was amplified and cloned into pcDNA3.1 vector with Eco RI and Xba I sites. To generate the SRSF1 knockdown vector, designed sequence for producing SRSF1 short hairpin RNA was amplified and cloned into pMKO.1 vector with Age I and Eco RI sites. 293T cells were transfected with the SRSF1-expressing or knockdown plasmid together with indicated minigene plasmids using Lipofectamine 2000 (catalog no. 11668019, Life Technologies) following the manufacturer's instruction. The transfected cells were harvested for RNA and protein analyses 48 hours later. Semiquantitative PCR was performed with primers amplifying endogenous transcripts, and the relative DNA binds were further confirmed through sequencing.

BM chimeras and retroviral transduction

BM cells were isolated from control, *Srsf1*$^{fl/fl}$*Lck*$^{Cre/+}$ (CD45.2$^+$) mice, and B6.SJL (CD45.1$^+$) mice. The lethally irradiated (7.5 Gy) WT B6.SJL (CD45.1$^+$) mice were regarded as recipients. A 1:1 mixture of BM cells (a total of 4×10^6 cells) from control (CD45.2$^+$) and B6.SJL (CD45.1$^+$) mice or from *Srsf1*$^{fl/fl}$*Lck*$^{Cre/+}$ (CD45.2$^+$) mice and WT B6.SJL (CD45.1$^+$) mice was transferred into the irradiated recipients. Then, the recipients were continuously administered with antibiotic-containing water for 2 weeks. Eight to 10 weeks later, the recipients were analyzed.

BM cells from control or *Srsf1*$^{fl/fl}$*Lck*$^{Cre/+}$ mice were lineage-depleted and then infected with pMigR1 empty vector or *Irf7*-expressing pMig retrovirus. Briefly, the retrovirus-bearing *Irf7* cDNA or pMigR1 along with pCL^{eco} was packaged with 293T cells and collected at 48 and 72 hours. The retrovirus-containing medium was filtered by 0.45-μm filters and loaded onto non–tissue culture 24-well plates (catalog no. 351147, Falcon), which were precoated with RetroNectin (10 μg/ml; catalog no. T100A, TaKaRa) following the manufacturer's instruction. The lineage-depleted BM cells were cultured for 24 hours in Iscove's Modified Dulbecco's Medium (IMDM) [supplemented with streptomycin and penicillin (100 μg/ml), 50 μM 2-mercaptoethanol, 15% fetal bovine serum, thrombopoietin (20 ng/ml), and stem cell factor (50 ng/ml)] on the retrovirus-containing RetroNectin plate as described above. Then, the cells were spinofected at 1000 rcf for 90 min at 30°C in the presence of Polybrene (4 μg/ml; catalog no. H9268, Sigma-Aldrich). After spinofection, the cells were cultured at 37°C in 5% CO_2 incubator for another 2 hours and then replaced with full IMDM medium containing components and cytokines as above for 24 to 48 hours. The infected lineage-negative BM cells containing 2000 to 5000 GFP$^+$ Lin$^-$Sca1$^+$c-Kit$^+$ (LSK) cells were then transplanted into irradiated B6.SJL mice at the dosage of 7.5 Gy. The recipients were analyzed at 8 to 10 weeks after transplantation.

RNA-seq and data analysis

TCRβ^{hi} DP cells were sorted from control and *Srsf1*$^{fl/fl}$*Lck*$^{Cre/+}$ mice, and the total RNAs were extracted following the protocol as described above. The quality of RNA samples was examined by a 2100 pico chip on the Bioanalyzer (Agilent). The high-quality RNAs were used to prepare the libraries, followed by high-throughput sequencing on an Illumina Xten platform with 150-bp paired-end reads.

For the RNA-seq data analysis, raw reads and adapter sequences were checked using FastQC (version 0.11.5). Cutadapt (version 1.17) and trim galore (version 0.6.0) were used to filter low-quality bases and artifacts. Next, clean reads were mapped to the mm10 reference genome using STAR (version 2.6). HTSeq (version 0.6.1) was used to count RNA-seq reads at gene level with parameters "-f bam -r name -a 10 -t exon -s no -i gene_id -m union." Subsequently, DESeq2 (version 1.20.0) was applied on gene counts to identify DEGs between control and *Srsf1*$^{fl/fl}$*Lck*$^{Cre/+}$ samples after removing zero counts in all replicates. DEGs were identified between the two groups at a *P* value of <5% and absolute $\log_2$FoldChange $\geq$ 0.6. The quality of replicates was assessed by calculating the pairwise Spearman correlation coefficient. Meanwhile, the expression values normalized by fragments per kilobase million (FPKM) are presented as a heatmap.

AS analysis

To identify the differentially alternative splicing events due to ablation of SRSF1, rMATS (version 4.0.2) software was used to calculate inclusion levels for different types of AS events: SEs, RIs, MXEs, A5SSs, and A3SSs in samples from control or *Srsf1*$^{fl/fl}$*Lck*$^{Cre/+}$ cells. Then, the differences were calculated by subtracting the inclusion levels in control mice from those in *Srsf1*$^{fl/fl}$*Lck*$^{Cre/+}$ samples. Splicing events with a false discovery rate (FDR) of <0.001 and the inclusion-level difference greater than 5% (0.05) were considered as statistically significant. Sashimi plots in IGV (version 2.8.10) were used to visualize and confirm events of AS in RNA-seq data.

irCLIP-seq and data analysis

Total thymocytes were isolated from WT C57BL/6 mice, and then the cells were cross-linked by ultraviolet light (254 nm) to maintain covalent binding of RBPs to their cognate RNA. Subsequently, the SRSF1 and cross-linked RNAs were immunoprecipitated with anti-SRSF1 antibody and digested with Micrococcal nuclease (catalog no. EN0181, Thermo Fisher Scientific). An IR800-biotin adapter was ligated to the 3′ end of the RNA fragment. Then, the SRSF1/RNA complexes were separated by SDS-PAGE gel and transferred to the nitrocellulose membrane (catalog no. HATF00010, Millipore). These RNA and protein complexes from about 47 to 62 kDa were extracted from the nitrocellulose membrane and followed by proteinase K (catalog no. 9034, TaKaRa) digestion. RNAs were isolated with saturated phenol (catalog no. AM9712, Ambion), ligated with adaptors, and converted to cDNAs by the SuperScript III First-Strand Kit (catalog no. 18080-051, Invitrogen). cDNAs were amplified by PCR to prepare the relative libraries and then sequenced on the HiSeq 2500 Illumina platform.

For the analysis of CLIP-seq data, the reads were first trimmed of adaptor sequences by Trimmomatic (version 0.36). Subsequently, bowtie 2 (version 2.1.0) was applied for mapping clean reads to the mm10 reference genome with parameters "-p 10 -L 15 -N 1 -D 50 -R 50 --phred33 --qc-filter --very-sensitive --end-to-end." CLIP-seq peaks were identified by Piranha (version 1.2.1) with the following parameters: "-s -b 20 -d Zero Truncated Negative Binomial -p 0.05." Homer (version 4.9.1) was used for peak annotation based on the mm10 genome assembly and for analysis of SRSF1-binding motifs. The quality of replicates was assessed by calculating the pairwise Spearman correlation coefficient.

GO and GSEA analysis

GO and pathway analysis were carried out using the online database String (version 10.5) with the default mouse genome as background and R package clusterProfiler (version 3.12.0). The mouse genome data were used as the reference, and Benjamini-Hochberg multiple tests were applied for adjustment of multiple testing. Functional category terms with an FDR of no more than 0.05 were regarded as significant categories. GSEA (version 3.0) (www.broadinstitute.org/gsea/downloads.jsp) was performed with default settings, and gene sets were selected from GSEA database. The relative gene expression profiles were used as the input dataset. Enrichment was considered significant at an FDR of ≤0.1 and the nominal *P* value of ≤0.05.

Regulatory network analysis

Network analysis was visualized using Cytoscape software (3.7.2). We first computed the AS genes and DEGs by RNA-seq data and the SRSF1-binding genes by CLIP-seq data for further analysis. We used the regulation of selected genes as input into the Cytoscape. Border color for each gene represented the AS or not. Fill color of nodes indicated the gene expression, which was up-regulated or

down-regulated. The edges between SRSF1 and other nodes represented the binding events.

Statistical analysis

GraphPad Prism software (version 8.0) was used to perform statistical analysis. The statistical significances were determined with Student's *t* test. A *P* value of less than 0.05 was considered statistically significant (*$P < 0.05$, **$P < 0.01$, and ***$P < 0.001$; ns denotes not statistically significant throughout the paper). Additional details about sample size and statistical tests used in different experiments can be found in the figure legends.

SUPPLEMENTARY MATERIALS

Supplementary material for this article is available at http://advances.sciencemag.org/cgi/content/full/7/16/eabf0753/DC1

REFERENCES AND NOTES

1. E. V. Rothenberg, J. E. Moore, M. A. Yui, Launching the T-cell-lineage developmental programme. *Nat. Rev. Immunol.* **8**, 9–21 (2008).
2. H. S. Teh, P. Kisielow, B. Scott, H. Kishi, Y. Uematsu, H. Blüthmann, H. von Boehmer, Thymic major histocompatibility complex antigens and the αβ T-cell receptor determine the CD4/CD8 phenotype of T cells. *Nature* **335**, 229–233 (1988).
3. A. Singer, S. Adoro, J. H. Park, Lineage fate and intense debate: Myths, models and mechanisms of CD4- versus CD8-lineage choice. *Nat. Rev. Immunol.* **8**, 788–801 (2008).
4. M. S. Jordan, A. Boesteanu, A. J. Reed, A. L. Petrone, A. E. Holenbeck, M. A. Lerman, A. Naji, A. J. Caton, Thymic selection of $CD4^+CD25^+$ regulatory T cells induced by an agonist self-peptide. *Nat. Immunol.* **2**, 301–306 (2001).
5. K. A. Hogquist, Y. Xing, F. C. Hsu, V. S. Shapiro, T cell adolescence: Maturation events beyond positive selection. *J. Immunol.* **195**, 1351–1357 (2015).
6. H. Kishimoto, J. Sprent, Negative selection in the thymus includes semimature T cells. *J. Exp. Med.* **185**, 263–272 (1997).
7. J. E. Cowan, N. I. McCarthy, S. M. Parnell, A. J. White, A. Bacon, A. Serge, M. Irla, P. J. L. Lane, E. J. Jenkinson, W. E. Jenkinson, G. Anderson, Differential requirement for CCR4 and CCR7 during the development of innate and adaptive αβT cells in the adult thymus. *J. Immunol.* **193**, 1204–1212 (2014).
8. R. Jin, W. Wang, J.-Y. Yao, Y.-B. Zhou, X.-P. Qian, J. Zhang, Y. Zhang, W.-F. Chen, Characterization of the in vivo dynamics of medullary $CD4^+CD8^-$ thymocyte development. *J. Immunol.* **180**, 2256–2263 (2008).
9. X. Xu, S. Zhang, P. Li, J. Lu, Q. Xuan, Q. Ge, Maturation and emigration of single-positive thymocytes. *Clin. Dev. Immunol.* **2013**, 282870 (2013).
10. F. C. Steinke, S. Yu, X. Zhou, B. He, W. Yang, B. Zhou, H. Kawamoto, J. Zhu, K. Tan, H.-H. Xue, TCF-1 and LEF-1 act upstream of Th-POK to promote the $CD4^+$ T cell fate and interact with Runx3 to silence *Cd4* in $CD8^+$ T cells. *Nat. Immunol.* **15**, 646–656 (2014).
11. M. Matloubian, C. G. Lo, G. Cinamon, M. J. Lesneski, Y. Xu, V. Brinkmann, M. L. Allende, R. L. Proia, J. G. Cyster, Lymphocyte egress from thymus and peripheral lymphoid organs is dependent on S1P receptor 1. *Nature* **427**, 355–360 (2004).
12. I. Aifantis, M. Mandal, K. Sawai, A. Ferrando, T. Vilimas, Regulation of T-cell progenitor survival and cell-cycle entry by the pre-T-cell receptor. *Immunol. Rev.* **209**, 159–169 (2006).
13. U. Koch, F. Radtke, Mechanisms of T cell development and transformation. *Annu. Rev. Cell Dev. Biol.* **27**, 539–562 (2011).
14. S. Gerondakis, T. S. Fulford, N. L. Messina, R. J. Grumont, NF-κB control of T cell development. *Nat. Immunol.* **15**, 15–25 (2014).
15. Y. Xing, X. Wang, S. C. Jameson, K. A. Hogquist, Late stages of T cell maturation in the thymus involve NF-κB and tonic type I interferon signaling. *Nat. Immunol.* **17**, 565–573 (2016).
16. S. Das, A. R. Krainer, Emerging functions of SRSF1, splicing factor and oncoprotein, in RNA metabolism and cancer. *Mol. Cancer Res.* **12**, 1195–1204 (2014).
17. T. Katsuyama, H. Li, D. Comte, G. C. Tsokos, V. R. Moulton, Splicing factor SRSF1 controls T cell hyperactivity and systemic autoimmunity. *J. Clin. Invest.* **129**, 5411–5423 (2019).
18. X. Xu, D. Yang, J. H. Ding, W. Wang, P. H. Chu, N. D. Dalton, H. Y. Wang, J. R. Bermingham Jr., Z. Ye, F. Liu, M. G. Rosenfeld, J. L. Manley, J. Ross Jr., J. Chen, R. P. Xiao, H. Cheng, X. D. Fu, ASF/SF2-regulated CaMKIIdelta alternative splicing temporally reprograms excitation-contraction coupling in cardiac muscle. *Cell* **120**, 59–72 (2005).
19. T. Hennet, F. K. Hagen, L. A. Tabak, J. D. Marth, T-cell-specific deletion of a polypeptide N-acetylgalactosaminyl-transferase gene by site-directed recombination. *Proc. Natl. Acad. Sci. U.S.A.* **92**, 12070–12074 (1995).
20. K. E. Chaffin, C. R. Beals, T. M. Wilkie, K. A. Forbush, M. I. Simon, R. M. Perlmutter, Dissection of thymocyte signaling pathways by in vivo expression of pertussis toxin ADP-ribosyltransferase. *EMBO J.* **9**, 3821–3829 (1990).
21. W. Cao, J. Guo, X. Wen, L. Miao, F. Lin, G. Xu, R. Ma, S. Yin, Z. Hui, T. Chen, S. Guo, W. Chen, Y. Huang, Y. Liu, J. Wang, L. Wei, L. Wang, CXXC finger protein 1 is critical for T-cell intrathymic development through regulating H3K4 trimethylation. *Nat. Commun.* **7**, 11687 (2016).
22. M. Zheng, D. Li, Z. Zhao, D. Shytikov, Q. Xu, X. Jin, J. Liang, J. Lou, S. Wu, L. Wang, H. Hu, Y. Zhou, X. Gao, L. Lu, Protein phosphatase 2A has an essential role in promoting thymocyte survival during selection. *Proc. Natl. Acad. Sci. U.S.A.* **116**, 12422–12427 (2019).
23. A. W. Goldrath, M. J. Bevan, Selecting and maintaining a diverse T-cell repertoire. *Nature* **402**, 255–262 (1999).
24. P. J. Fink, The biology of recent thymic emigrants. *Annu. Rev. Immunol.* **31**, 31–50 (2013).
25. T. E. Boursalian, J. Golob, D. M. Soper, C. J. Cooper, P. J. Fink, Continued maturation of thymic emigrants in the periphery. *Nat. Immunol.* **5**, 418–425 (2004).
26. S. Tani-ichi, A. Shimba, K. Wagatsuma, H. Miyachi, S. Kitano, K. Imai, T. Hara, K. Ikuta, Interleukin-7 receptor controls development and maturation of late stages of thymocyte subpopulations. *Proc. Natl. Acad. Sci. U.S.A.* **110**, 612–617 (2013).
27. T. M. McCaughtry, R. Etzensperger, A. Alag, X. Tai, S. Kurtulus, J. H. Park, A. Grinberg, P. Love, L. Feigenbaum, B. Erman, A. Singer, Conditional deletion of cytokine receptor chains reveals that IL-7 and IL-15 specify CD8 cytotoxic lineage fate in the thymus. *J. Exp. Med.* **209**, 2263–2276 (2012).
28. Y. Y. Wan, H. Chi, M. Xie, M. D. Schneider, R. A. Flavell, The kinase TAK1 integrates antigen and cytokine receptor signaling for T cell development, survival and function. *Nat. Immunol.* **7**, 851–858 (2006).
29. S. Pandit, Y. Zhou, L. Shiue, G. Coutinho-Mansfield, H. Li, J. Qiu, J. Huang, G. W. Yeo, M. Ares Jr., X. D. Fu, Genome-wide analysis reveals SR protein cooperation and competition in regulated splicing. *Mol. Cell* **50**, 223–235 (2013).
30. Q. Lin, C. Dong, M. D. Cooper, Impairment of T and B cell development by treatment with a type I interferon. *J. Exp. Med.* **187**, 79–87 (1998).
31. H. Tang, J. Zhang, X. Sun, X. Qian, Y. Zhang, R. Jin, Thymic DCs derived IL-27 regulates the final maturation of $CD4^+$ SP thymocytes. *Sci. Rep.* **6**, 30448 (2016).
32. D. J. Gough, N. L. Messina, C. J. Clarke, R. W. Johnstone, D. E. Levy, Constitutive type I interferon modulates homeostatic balance through tonic signaling. *Immunity* **36**, 166–174 (2012).
33. H. Yoshida, C. A. Hunter, The immunobiology of interleukin-27. *Annu. Rev. Immunol.* **33**, 417–443 (2015).
34. L. Frankiw, D. Majumdar, C. Burns, L. Vlach, A. Moradian, M. J. Sweredoski, D. Baltimore, BUD13 promotes a type I interferon response by countering intron retention in Irf7. *Mol. Cell* **73**, 803–814.e6 (2019).
35. N. Hug, D. Longman, J. F. Caceres, Mechanism and regulation of the nonsense-mediated decay pathway. *Nucleic Acids Res.* **44**, 1483–1495 (2016).
36. X. Zhou, R. Wang, X. Li, L. Yu, D. Hua, C. Sun, C. Shi, W. Luo, C. Rao, Z. Jiang, Y. Feng, Q. Wang, S. Yu, Splicing factor SRSF1 promotes gliomagenesis via oncogenic splice-switching of MYO1B. *J. Clin. Invest.* **129**, 676–693 (2019).
37. M. M. Maslon, S. R. Heras, N. Bellora, E. Eyras, J. F. Caceres, The translational landscape of the splicing factor SRSF1 and its role in mitosis. *eLife* **3**, e02028 (2014).
38. D. J. Zhang, Q. Wang, J. Wei, G. Baimukanova, F. Buchholz, A. F. Stewart, X. Mao, N. Killeen, Selective expression of the Cre recombinase in late-stage thymocytes using the distal promoter of the *Lck* Gene. *J. Immunol.* **174**, 6725–6731 (2005).
39. L. Klein, B. Kyewski, P. M. Allen, K. A. Hogquist, Positive and negative selection of the T cell repertoire: What thymocytes see (and don't see). *Nat. Rev. Immunol.* **14**, 377–391 (2014).
40. K. A. Hogquist, S. C. Jameson, The self-obsession of T cells: How TCR signaling thresholds affect fate 'decisions' and effector function. *Nat. Immunol.* **15**, 815–823 (2014).
41. B. Seddon, Thymic IL-7 signaling goes beyond survival. *Nat. Immunol.* **16**, 337–338 (2015).
42. M. Pellegrini, P. Bouillet, M. Robati, G. T. Belz, G. M. Davey, A. Strasser, Loss of Bim increases T cell production and function in interleukin 7 receptor-deficient mice. *J. Exp. Med.* **200**, 1189–1195 (2004).
43. J. C. Rathmell, T. Lindsten, W. X. Zong, R. M. Cinalli, C. B. Thompson, Deficiency in Bak and Bax perturbs thymic selection and lymphoid homeostasis. *Nat. Immunol.* **3**, 932–939 (2002).
44. C. Dong, A. E. Juedes, U. A. Temann, S. Shresta, J. P. Allison, N. H. Ruddle, R. A. Flavell, ICOS co-stimulatory receptor is essential for T-cell activation and function. *Nature* **409**, 97–101 (2001).
45. I. Kleiter, J. Song, D. Lukas, M. Hasan, B. Neumann, A. L. Croxford, X. Pedré, N. Hövelmeyer, N. Yogev, A. Mildner, M. Prinz, E. Wiese, K. Reifenberg, S. Bittner, H. Wiendl, L. Steinman, C. Becker, U. Bogdahn, M. F. Neurath, A. Steinbrecher, A. Waisman, Smad7 in T cells drives T helper 1 responses in multiple sclerosis and experimental autoimmune encephalomyelitis. *Brain* **133**, 1067–1081 (2010).
46. N. C. Douglas, H. Jacobs, A. L. Bothwell, A. C. Hayday, Defining the specific physiological requirements for c-Myc in T cell development. *Nat. Immunol.* **2**, 307–315 (2001).

47. E. Woolf, C. Xiao, O. Fainaru, J. Lotem, D. Rosen, V. Negreanu, Y. Bernstein, D. Goldenberg, O. Brenner, G. Berke, D. Levanon, Y. Groner, Runx3 and Runx1 are required for CD8 T cell development during thymopoiesis. *Proc. Natl. Acad. Sci. U.S.A.* **100**, 7731–7736 (2003).
48. M. Lohoff, H. W. Mittrücker, A. Brüstle, F. Sommer, B. Casper, M. Huber, D. A. Ferrick, G. S. Duncan, T. W. Mak, Enhanced TCR-induced apoptosis in interferon regulatory factor 4-deficient $CD4^+$ Th cells. *J. Exp. Med.* **200**, 247–253 (2004).
49. Y. M. Kerdiles, D. R. Beisner, R. Tinoco, A. S. Dejean, D. H. Castrillon, R. A. DePinho, S. M. Hedrick, Foxo1 links homing and survival of naive T cells by regulating L-selectin, CCR7 and interleukin 7 receptor. *Nat. Immunol.* **10**, 176–184 (2009).
50. H. Suzuki, T. Kundig, C. Furlonger, A. Wakeham, E. Timms, T. Matsuyama, R. Schmits, J. Simard, P. Ohashi, H. Griesser, Deregulated T cell activation and autoimmunity in mice lacking interleukin-2 receptor beta. *Science* **268**, 1472–1476 (1995).
51. I. M. de Alboran, R. C. O'Hagan, F. Gärtner, B. Malynn, L. Davidson, R. Rickert, K. Rajewsky, R. A. DePinho, F. W. Alt, Analysis of C-MYC function in normal cells via conditional gene-targeted mutation. *Immunity* **14**, 45–55 (2001).
52. A. Metidji, S. A. Rieder, D. D. Glass, I. Cremer, G. A. Punkosdy, E. M. Shevach, IFN-α/β receptor signaling promotes regulatory T cell development and function under stress conditions. *J. Immunol.* **194**, 4265–4276 (2015).
53. N. Hata, M. Sato, A. Takaoka, M. Asagiri, N. Tanaka, T. Taniguchi, Constitutive IFN-α/β signal for efficient *IFN-α/β* gene induction by virus. *Biochem. Biophys. Res. Commun.* **285**, 518–525 (2001).
54. K. Honda, A. Takaoka, T. Taniguchi, Type I interferon [corrected] gene induction by the interferon regulatory factor family of transcription factors. *Immunity* **25**, 349–360 (2006).
55. D. C. Otero, D. P. Baker, M. David, IRF7-dependent IFN-β production in response to RANKL promotes medullary thymic epithelial cell development. *J. Immunol.* **190**, 3289–3298 (2013).

Acknowledgments: We thank R. Jin (Department of Immunology, NHC Key Laboratory of Medical Immunology, Peking University) for discussions and technical assistance. We thank H.-H. Xue (Hackensack University Medical Center) for constructive suggestions and manuscript modification. We thank X. Zhou (Third Military Medical University) for sharing multiple plasmids and technical support. We thank B. Zhang at the Laboratory Animal Center in China Agricultural University for assistance of animal care. **Funding:** This work was supported in part by the National Key R&D Program of China (2017YFA0104401) to S.Y., National Natural Science Foundation of China (31970831, 31630038, and 31571522) to S.Y., and the Project for Extramural Scientists supported by the State Key Laboratory of Agrobiotechnology of China Agricultural University (2018SKLAB6-30, 2019SKLAB6-6, and 2019SKLAB6-7). **Author contributions:** Z.Q., F.W., and G.Y. performed the major experiments and analyzed overall experimental data. D.W. performed the CLIP-seq and helped Z.Q. perform the minigene assay in vitro. F.W. and M.Y. analyzed and presented the high-throughput data. Jingjing Liu, Y.Y., Juanjuan Liu, Z.S., C.J., Y.X., and S.Y. assisted the overall experiments and interpreted data. S.Y. designed and supervised the experiments. S.Y., Z.Q., and F. W. wrote the manuscripts with modifications from all authors. **Competing interests:** The authors declare that they have no competing interests. **Data and materials availability:** All data needed to evaluate the conclusions in the paper are present in the paper and/or the Supplementary Materials. CLIP-seq and RNA-seq data that are reported in this study have been deposited in the GEO database with series accession number GSE141349. Additional data related to this paper may be requested from the authors.

Submitted 1 October 2020
Accepted 25 February 2021
Published 16 April 2021
10.1126/sciadv.abf0753

Citation: Z. Qi, F. Wang, G. Yu, D. Wang, Y. Yao, M. You, J. Liu, J. Liu, Z. Sun, C. Ji, Y. Xue, S. Yu, SRSF1 serves as a critical posttranscriptional regulator at the late stage of thymocyte development. *Sci. Adv.* **7**, eabf0753 (2021).